Accepted Manuscript

Western Paraná suture/shear zone and the limits of Rio Apa, Rio Tebicuary and Rio de la Plata cratons from gravity data

Gabriel Negrucci Dragone, Naomi Ussami, Mario Ernesto Gimenez, Federico Gustavo Lince Klinger, Carlos Alberto Moreno Chaves

PII: S0301-9268(16)30106-1
DOI: http://dx.doi.org/10.1016/j.precamres.2017.01.029
Reference: PRECAM 4662

To appear in: *Precambrian Research*

Received Date: 2 May 2016
Revised Date: 28 January 2017
Accepted Date: 30 January 2017

Title

Western Paraná suture/shear zone and the limits of Rio Apa, Rio Tebicuary and Rio de la Plata cratons from gravity data

Authors

Gabriel Negrucci Dragone[a,*], Naomi Ussami[a], Mario Ernesto Gimenez[b], Federico Gustavo Lince Klinger[b], Carlos Alberto Moreno Chaves[a]

[a] Instituto de Astronomia, Geofísica e Ciências Atmosféricas, Departamento de Geofísica, Universidade de São Paulo, Rua do Matão, 1226, 05508-090, São Paulo, Brazil. E-mails: gabriel.dragone@usp.br, nussami@usp.br, carlos.chaves@iag.usp.br

[b] CONICET, Instituto Geofísico Sismológico Volponi (IGSV), Facultad de Ciencias Exactas, Físicas y Naturales, Universidad Nacional de San Juan, Ruta 12, km 17 (Jardín de los Poetas) C.P. 5407, Marquesado, San Juan, Argentina. E-mails: mgimenez@UNSJ-cuim.edu.ar, flinceklinger@gmail.com

[*]Corresponding author. E-mail: gabriel.dragone@usp.br

Abstract

We present a new gravity map between 45°-70° W and 5°-40° S integrating open source terrestrial gravity data of Argentina with the South American Gravity Model 2004 (SAGM04), a 5 min-arc resolution gravity model. The Bouguer anomaly map reveals a 2,000 km long linear gravity feature from 15° S to 30° S at longitude 55° W, with a steep horizontal gradient separating two gravity domains. The eastern domain is the Paraná basin, with NE-SW trending Bouguer anomalies of -80 mGal in average. The western domain comprises the Chaco-Paraná, Chaco-Tarija and Pantanal basins, with circular positive anomalies of up to 20 mGal in amplitude. Previous seismic studies mapped a thinner crust of less than 35 km in the western domain and the present gravity models indicate a 10 to 20 kg/m³ denser crust. On the other hand, the eastern domain has a thicker crust of more than 40 km. Seismic tomography models also show P- and S-wave velocity reduction in the western domain whereas high-velocity characterises the Paraná basin. These geophysical data indicate that the gravity gradient marks a transition between two distinct lithospheres. The gravity gradient is associated with a tectonic feature referred to as the Western Paraná suture/shear zone. Granites of 530 to 570 Ma ages, located parallel or over the gravity gradient, suggest a Neoproterozoic to Early Cambrian age suture/shear zone, thus approximately synchronous and parallel to the Pampean belt. Sediment corrected residual gravity map and its vertical derivative allow us to define the limits of the Rio Apa, Rio de la Plata and Rio Tebicuary cratons. Their eastern and western limits are the Western Paraná suture and the Pampean belt, respectively. This study unravels Precambrian tectonic elements concealed by the Phanerozoic sedimentary basins adding new constraints for the amalgamation history of SW Gondwana.

Research Highlights

Gravity map reveals the Neoproterozoic 2,000 km long Western Paraná suture/shear zone

Geophysical delimitation of the Rio Apa, Rio Tebicuary and Rio de la Plata cratons

Gravity anomalies of the Amazonian and Rio Apa cratons are distinct

New tectonic features of SW Gondwana final amalgamation revealed

Key Words

SW Gondwana; intracontinental basins; cratons; sutures; gravity

1. Introduction

A major advance in understanding the Neoproterozoic to Cambrian tectonic history of the SW Gondwana supercontinent evolution has been achieved in the last decade with the acquisition of new geochronological data (Ar-Ar and U-Pb ages) and isotope geochemistry studies of igneous and metamorphic rocks of the exposed basement of cratons and ancient terranes (Cordani *et al.*, 2001; Rapela *et al.*, 2007; Cordani *et al.*, 2010; Oyhantçabal *et al.*, 2010; Escayola et al, 2011; Rapela *et al.*, 2011; Casquet *et al.*, 2012). Together with a few paleomagnetic (Trindade *et al.*, 2006; Tohver *et al.*, 2010; Rapalini *et al.*, 2013) and sediment provenance studies using zircon detritus ages and the geochronology of Neoproterozoic Pampean back-arc basins (Rapela *et al.*, 1998, Rapela *et al.*, 2007, Escayola *et al.*, 2007, Rapela *et al.*, 2011, Ramos *et al.*, 2015) and of the Paraguay orogenic belt (Bandeira *et al.*, 2012; Babinski et al, 2013; McGee *et al.*, 2015), a new view of the final amalgamation of the SW Gondwana is emerging.

Essential to the advancement of the Precambrian history of the SW Gondwana is the definition of the main tectonic units and their limits. Difficulties arise due to the post-Cambrian sedimentary sequences that cover more than 70% of the southwestern South America basement. These Phanerozoic sedimentary deposits are the intracontinental Paraná, Chaco-Paraná, Chaco-Tarija, Parecis and Pantanal basins (Fig. 1). Therefore, to unravel the Precambrian basement history, geophysical data are essential, and the number of regional and lithosphere scale geophysical studies in South America has progressively increased in the last decade. We use gravity data and integrate them with other available geophysical data such as magnetotellurics in Argentina (Favetto *et al.*, 2008, 2015; Orozco *et al.*, 2013; Peri *et al.*, 2013, 2015) and Brazil (Bologna *et al.*, 2014; Padilha *et al.,* 2015), and regional seismological studies (Feng *et al.*, 2007; Assumpção *et al.*, 2013; Rosa *et al.* 2016). This integration provides a more robust lithospheric physical model for this segment of the South American plate.

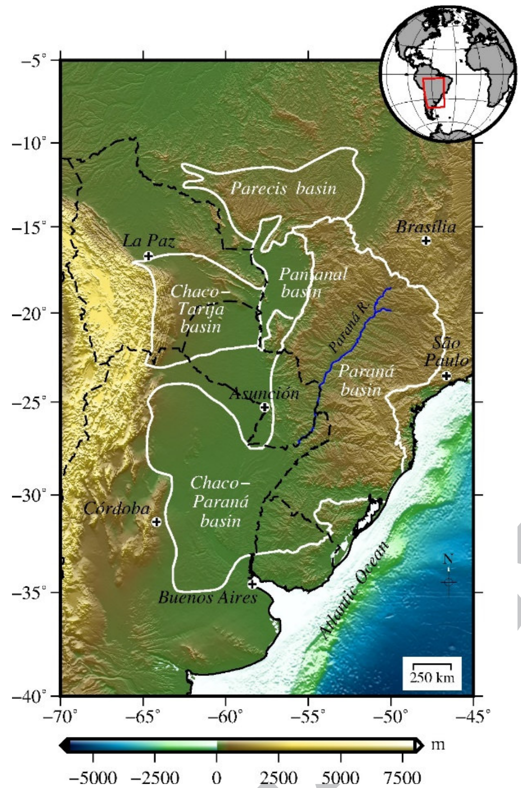

Figure 1 – Topographic map (ETOPO1, Amante and Eakins, 2009) of the study area. Dashed lines are the political limits of Brazil, Uruguay, Paraguay, Argentina and Bolivia. Continuous white contours are the limits of the Paraná, Chaco-Paraná, Chaco-Tarija, Pantanal and Parecis sedimentary basins. The continuous blue line is the Paraná River.

For lithospheric scale tectonic studies, good resolution global gravity models are available thanks to several satellite gravity missions integrated with conventional terrestrial gravity surveys. One of such a model is the EGM08 (**E**arth **G**ravitational **M**odel, Pavlis *et al.*, 2012), a 5 min-arc resolution model which combines terrestrial gravity and GRACE satellite data. However, the documentation on the source of the South American terrestrial gravity data used for constructing the EGM08 model is not readily accessible. Therefore, some caution is required when using this model for regional scale tectonic studies in South America, as discussed by Bomfim *et al.* (2013) for the Amazonian craton region.

We integrate the SAGM04 model (**S**outh **A**merican **G**ravity **M**odel 2004) by Sá (2004) with the open access data over the Chaco-Paraná basin from the **I**nstituto **G**eográfico **N**acional (IGN) of Argentina. To accomplish it, we use the most recent gravity model entirely derived from GOCE data (**G**ravity field and steady-state **O**cean **C**irculation **E**xplorer, ESA, 1999; Bruinsma *et al.*, 2013), which allow us to tie all gravity measurements to the same reference system and to evaluate the IGN data quality.

Three results from the present gravity study are the most relevant. First, we identify a 2000 km long Neoproterozoic-Early Cambrian lithospheric suture/shear zone along the western border of the Paraná basin. Second, we propose that the Archean/ Paleoproterozoic age continental crust (Cordani *et al.*, 2001) under the Chaco-Paraná basin (between 65° W to 55° W longitude and 30° S to 35° S latitude) to be a new tectonic and cratonic unit, hereafter referred to as the Rio Tebicuary craton. The suture/shear zone separates the Rio Tebicuary, Rio de la Plata (Ramos, 1988, Rapela *et al.*, 2007, 2011) and Rio Apa (Cordani *et al.*, 2010) cratons from the Paraná basin lithosphere. Finally, positive gravity anomalies characterise these three cratons whereas negative gravity anomalies are predominant in the Amazonian and African cratons suggesting distinct crustal and lithospheric thickness and composition.

2. Gravity Map

We present a new gravity anomaly map between 45° W to 70° W in longitude and 5° S to 40° S in latitude (Fig. 2b), which results from the integration of IGN terrestrial data (Fig. 2a, blue dots) in Argentina and the South American regional model, the SAGM04 (Fig. 2a, green).

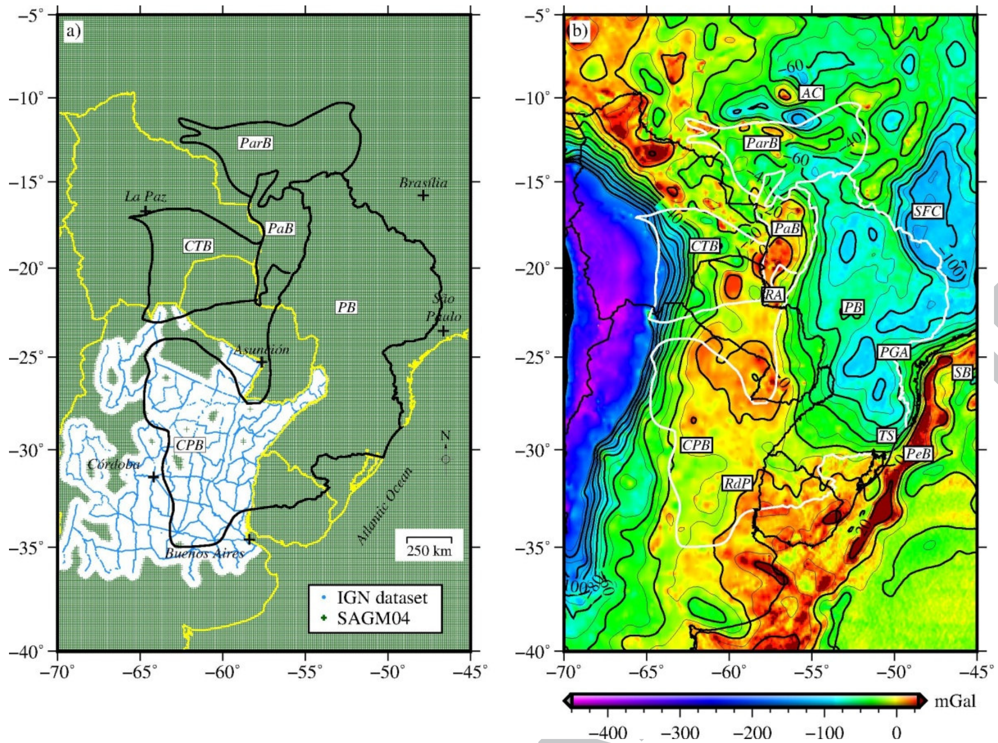

Figure 2 – a) Data used to compose the new gravity map. The IGN dataset is in blue dots. The SAGM04, a regular 5 min-arc grid, is in green and completes the Bouguer anomaly map. b) New gravity map, Bouguer anomalies over the continent and free-air over the ocean. Gravity anomalies in colour scale are at the geoid. Gravity anomalies upward continued to 30 km at 10 mGal contour interval. Tectonic units: AC – Amazonian craton; CPB – Chaco-Paraná basin; PaB – Pantanal basin; ParB – Parecis basin; PB – Paraná basin; PeB – Pelotas basin; PGA – Ponta Grossa arch; RA – Rio Apa craton; RdP – Rio de la Plata craton; SB – Santos basin; SFC – São Francisco craton; TS – Torres syncline.

Sá (2004) elaborated the SAGM04 gravity model integrating Brazilian terrestrial gravity data collected by several institutions and open access gravity data from neighbouring countries (supplementary material, Fig. S1). The SAGM04 lateral resolution is a 5 min-arc in areas with good terrestrial coverage. In regions devoid of terrestrial data, the EGM96 (**E**arth **G**ravitational **M**odel 1996, Lemoine *et al.*, 1998) and GPM98C (**G**ravitational **P**otential **M**odel 1998 C, Wenzel *et al.*, 1998) were used with an estimated lateral resolution of 30 min-arc and 15 min-arc, respectively. Due to a denser and larger terrestrial and marine dataset used, the SAGM04 is so far the best regional gravity model for most parts of South America.

"Insert Supplementary Figure S1 here"

The Argentina IGN dataset comprises 7509 gravity and orthometric altitude measurements. The latitude correction was carried out using the 1980 Geodetic Reference System ellipsoid (GRS80) (Moritz, 1984) and calculating the theoretical gravity on each station coordinates using Somigliana's formula (Somigliana, 1930, *apud* Moritz, 1980). The Bouguer correction was determined using a density of 2670 kg/m³. Figures S2 and S3 (supplementary material) describe the homogenisation and integration of the IGN gravity data into the SAGM04 model.

"Insert Supplementary Figures S2 and S3 here"

The final gravity data set comprises the SAGM04 model in areas inside Argentina where no terrestrial data were available within a 50 km radius (Fig. 2(a)). The gravity map shown in Fig. 2(b) comprises Bouguer anomalies over the continent and free-air anomalies over the ocean, with a lateral resolution of 5 min-arc. The digital map interpolation uses a splines in tension routine (Smith and Wessel, 1990) available in the GMT package (Wessel and Smith, 1991). Gravity anomalies referred to the geoid are in colour whereas the contour lines at 10 mGal interval are the gravity anomalies upward continued to 30 km height.

The upward continued gravity field suppresses short wavelength anomalies and highlight regional gravity features. In order to correlate the main gravity features with main geologic units, the upward continued gravity field was superimposed to a regional geological map, as shown in Fig. 3.

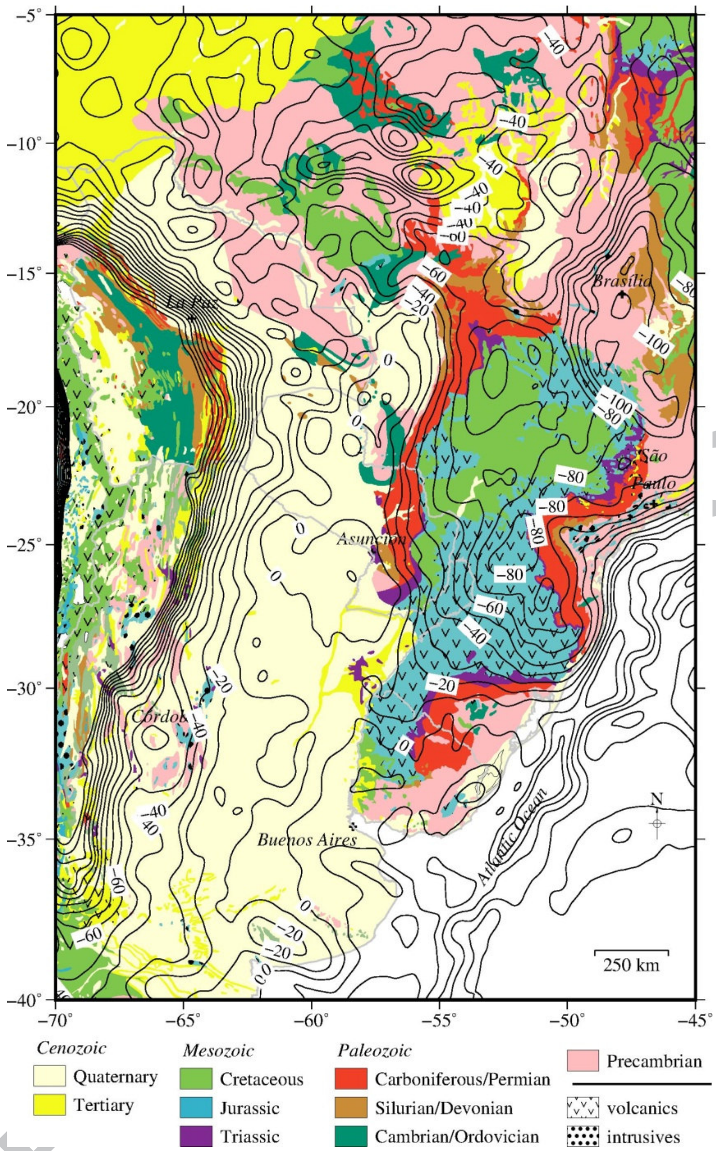

Figure 3 – Geological map adapted from the USGS (Schenk *et al.*, 1999) with upward continued (30 km) observed gravity anomaly map with contours at 10 mGal interval.

3. Gravity map analysis and modelling

3.1. Main gravity domains in the continent

The gravity map (Fig. 2(b) and Fig. 3) is divided into four main gravity provinces, from west to east: (i) negative Bouguer anomalies in the main Andean chain (< -80 mGal), (ii) a high gravity gradient (-80 to -20 mGal) associated with the sub-Andean basins and terranes, (iii) predominantly positive Bouguer anomalies (-20 to 20 mGal) in the Rio de la Plata and Rio Apa cratons, Chaco-Paraná, Chaco-Tarija and Pantanal basins and (iv) negative anomalies ranging between -120 and -40 mGal in the Paraná basin and south of Amazonian and São Francisco cratons. The main gravity feature is a linear N-S trending gravity gradient starting at latitude 15° S, south of the Amazonian craton and to the east of the Pantanal basin, and extending southwards, approximately following the 55° W meridian. At 30° S, this gradient bends to the east and extends towards the Torres syncline, terminating at the continental margin between Pelotas and Santos basins. The gradient is steeper (0.36 mGal/km) between the Pantanal and Paraná basins, and it is gentler (0.13 to 0.24 mGal/km) in its southwest and southern segments, where the Paraná basin is in contact, respectively, with the Chaco-Paraná basin and the Rio de la Plata craton.

To the west of the gradient, in the Pantanal and Chaco-Paraná basins, circular gravity highs varying in size and amplitude are dominant. In the Paraná basin, negative gravity anomalies are observed parallel to the Paraná River, where a NE-SW trending gravity high separates two gravity sub-domains. To the west, the gravity anomalies are negative and elongated along the N-NE direction, whereas to the east anomalies are variable in shape and separated by the Ponta Grossa arch (PGA in Fig. 2(b)). The short-wavelength gravity anomalies are due to a heterogeneous crust with variable composition and/or thickness (see discussion in section 3.4).

Parecis basin, situated in the southern portion of the Amazonian craton and north of Pantanal and Paraná basins (Fig. 2 and Fig. 3), is characterised by east-west trending negative gravity anomalies.

3.2. **Gravity effect due to Moho depth variation**

In order to evaluate if the observed expressive gravity gradient on the western border of the Paraná basin may be entirely due to changes in crustal thickness, we compiled seismological crust thickness estimates in the study area. A thinner crust (28-35 km) is observed in the Pantanal, Chaco-Tarija and Chaco-Paraná basins whereas a thicker crust (38-46 km) is systematically found in the Paraná basin (Assumpção *et al.*, 2013; Chulick *et al.*, 2013), as shown in Fig. 4(a). Moho depths estimated from seismic study are missing in large segments of the Chaco-Tarija, Chaco-Paraná and Pantanal basins. Thus, for these areas, we estimate the crustal thickness considering a local (Airy) compensation model of the observed topography. We use a globally estimated crust-mantle average depth of 35 km at sea level and a density contrast of 400 kg/m^3 between lower crust and upper mantle (Dziewonski and Anderson, 1981; Martinec, 1994). This simple isostatic model predicts crustal thicknesses in the sub-Andes, Rio de la Plata and Amazonian cratons and Chaco-Paraná basin within the estimated uncertainty (±2 to ±4 km) of the seismological study of Assumpção *et al.* (2013) wherever available. The calculation of the gravity effect due to Moho depth variation (Fig. 4(a)) uses rectangular prisms of variable heights (Nagy *et al.*, 2000) and follows the same procedure computationally implemented by Chaves and Ussami (2013).

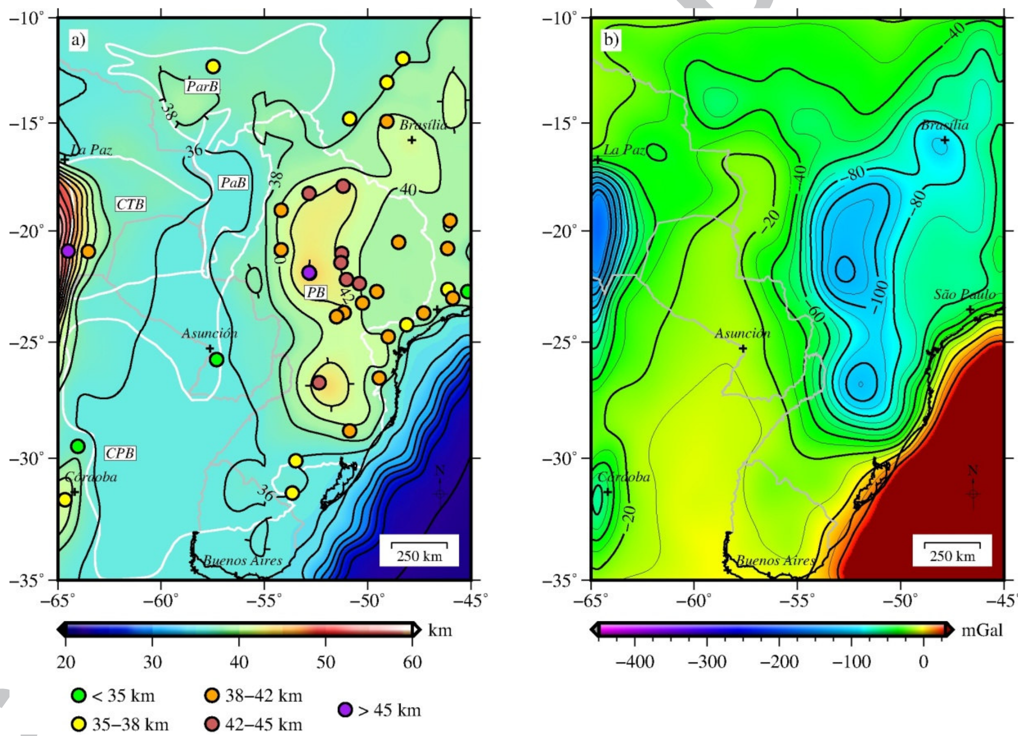

Figure 4 – a) Crustal thickness map. White continuous lines are the limits of the intracontinental basins. Contour interval is 2 km. Coloured dots are from deep seismic refraction experiments, receiver function analyses, and surface-wave dispersion velocities estimates compiled by Assumpção *et al.* (2013). In areas devoid of Moho depth estimates, the crust-mantle boundary is derived from local isostasy of observed topography. b) Calculated gravity effect of crust-mantle depth variation shown in (a) at 10 mGal contour interval. See text for details.

The main conclusion from an initial analysis is that the gravity gradient separating the Paraná basin from the Chaco-Paraná, Chaco-Tarija and Pantanal basins is partially due to a major crustal or lithospheric discontinuity. In order to estimate the crustal thickness variation and the density structure across the observed gravity gradient, we have also removed the gravity effects owing to basalts and sedimentary rocks within the Paraná and Chaco-Paraná basins. We present this step in the following section.

3.3. Gravity effects due to sediments and basalts

Sedimentary rocks isopachs from the Paraná basin (Milani *et al.*, 1998) and the Chaco-Paraná basin (Pezzi and Mozetic, 1989) are in Fig. 5(a), together with basalt isopachs (Fig. 5(b)) from the Serra Geral formation compiled by Melfi *et al.* (1988). The information on sediments and basalts thicknesses is from an uneven and sparse distribution of wells drilled for oil exploration. Therefore, the isopachs were interpolated in a 10 min-arc grid. The gravity effect calculation was performed using the gravity formula for rectangular prisms (Nagy *et al.*, 2000). Two average density contrasts between sedimentary rocks and crust, of -50 kg/m^3 and -100 kg/m^3, and a density contrast of +180 kg/m^3 between basalts and crust were used to calculate the gravity effects shown in Fig. 5(c) and Fig. 5(d), respectively. Density contrasts of Paleozoic sedimentary rocks are from sonic logging of a deep well in the Paraná basin (Molina *et al.*, 1989). For the basaltic layer, we consider the average value of 2850 kg/m^3 as determined by Marques *et al.* (1984) for the Serra Geral Formation. The density of 2670 kg/m^3 is the average value for the upper crust. Figs. 5(c) and 5(d) show that the amplitude of the gravity effect due to sedimentary and volcanic rocks inside the Chaco-Paraná and the Paraná basins varies from -5 mGal to -20 mGal. The positive gravity anomalies of approximately 5 mGal amplitude observed on the eastern border of the Paraná basin are associated with a thicker basaltic layer underlain by a thinner sedimentary layer.

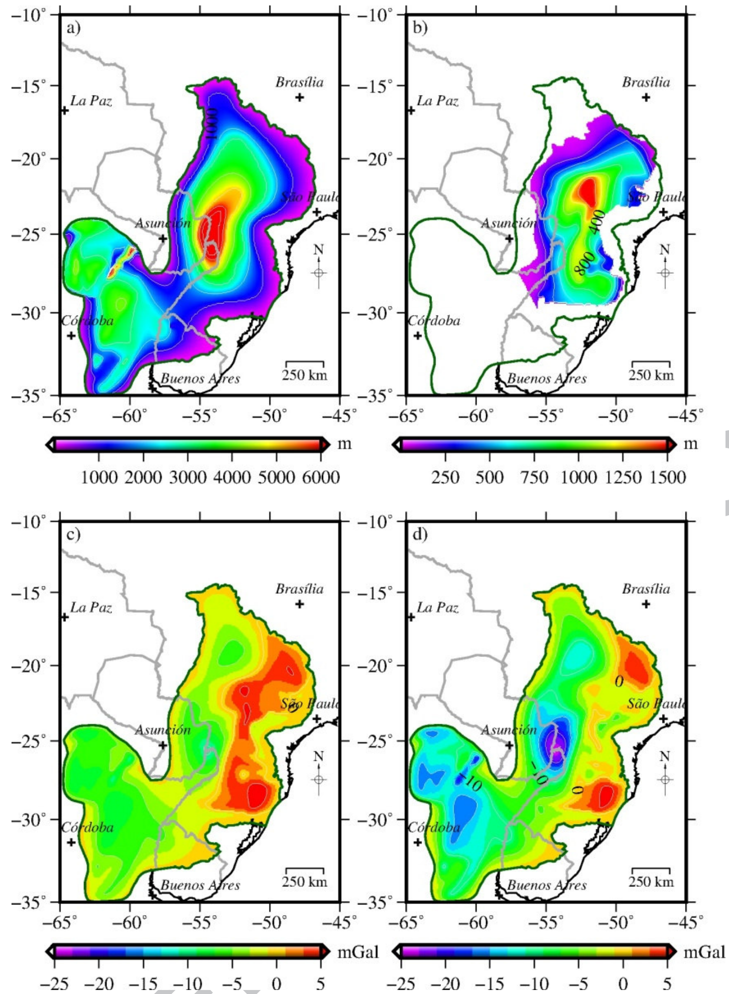

Figure 5 – a) Total sediment thickness; b) basalt thickness; c) gravity effect due to sediments and basalts using density contrasts between sedimentary rocks and crust of -50 kg/m^3 and d) -100 kg/m³. See text for details on gravity effect calculation.

The gravity effects shown in Fig. 5(c) and 5(d) were removed from the observed Bouguer anomalies at the geoid (Fig. 2(b)) and the results are shown in Figs. 6(a) and 6(b), respectively. Both are equally acceptable as residual gravity anomaly maps due to uncertainties in the average density contrasts between upper crust and sedimentary and basaltic rocks and the total thickness of both rock types. The goal was to estimate the regional gravity effects. Except for the amplitude of the gravity anomalies within these two sedimentary basins, no major change in the gravity signature of the gravity gradient is observed owing to this correction. Thus, its origin should be ascribed to crustal and/or lithospheric physical property variations, as also shown by seismological data.

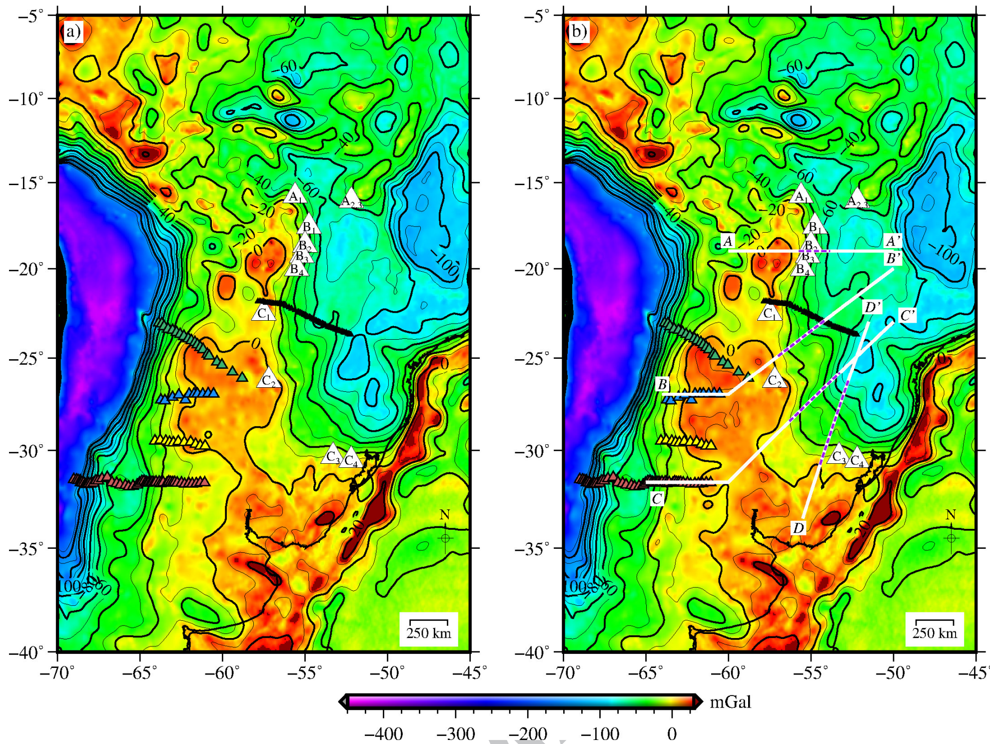

Figure 6 – Residual Bouguer gravity maps using density contrasts between sedimentary rocks and crust of a) -50 kg/m^3 and b) -100 kg/m³, and +180 kg/m^3 between basalts and crust for both cases. The modelled gravity profiles are highlighted in white, where the purple dashed lines correspond to the grey areas in the gravity models (profiles B-B' and C-C' are shown in Figs. 7 and 8; profiles A-A' and D-D' are shown as supplementary materials, Figs. S4 and S5). Coloured and black triangles are MT stations from several authors: to the west, green stations at latitude 23° S are from Favetto *et al.* (2015); blue stations at 27° S are from Peri *et al.* (2013); yellow stations at 29.5° S are from Peri *et al.* (2015); orange stations at 31.5° S are from Favetto *et al.* (2008) and Orozco *et al.* (2013); black stations at the Paraná basin are from Padilha *et al.* (2015). White triangles are the granites listed in Table 1 and discussed in Section 4.1.

3.4. Two-dimensional gravity forward modelling

In order to model the crustal structure across the gravity gradient, the crustal thickness and the effect of its variation on the gravity field (Fig. 4) are used as the main constraints for modelling the observed residual gravity anomalies.

Fig. 6(b) shows, in white straight lines, the location of the four gravity profiles taken from the residual gravity map. The profiles extend from west to east, starting in the sub-Andes and terminating in the centre or closer to the northern border of the Paraná basin. In Fig. 6, two additional data are presented. The first is the location of outcropping granitic bodies (white triangles). A letter and a number identify each granitic body with its geochronological dating method and age are summarised in Table 1. The second data are five magnetotelluric (MT) profiles with stations shown in coloured triangles. These additional geological and geophysical data appear in each crustal section derived from the gravity modelling.

Table 1 – List of granites of Neoproterozoic to Cambrian ages

Number	Name	Age (Ma)	Method	Reference
A1	São Vicente	504±8,9	U-Pb	Godoy *et al.*,2010
A2	Lajinha	505.4±4.1	U-Pb	Godoy *et al.*, 2010
A3	Araguaiana	509.4±2.2	U-Pb	Godoy *et al.*, 2010
B1	Sonora	548±5.9	U-Pb	Godoy *et al.*, 2010
B2	Coxim	540±3.6	U-Pb	Godoy *et al.*,2010
B3	Rio Negro	547±4.9	U-Pb	Godoy *et al.*, 2010
B4	Taboco	540±4.7	U-Pb	Godoy *et al.*, 2010
C1	San Ramon Suite	532±6	unknown	Wiens, 1986
C2	Caapucú Suite	531±5	Rb-Sr	Cubas *et al.*, 1998
C3	Caçapava do Sul	552±4	Rb-Sr	Sartori and Kawashita, 1985
C4	Dom Feliciano Suite	570-550	Rb-Sr	Phillip and Machado, 2005

Our gravity forward modelling is based on a computer algorithm for two-dimensional bodies of arbitrary polygonal cross-section (Talwani *et al.*, 1959). For crustal densities, we followed the IASP91 averages (Kennett, 1991): 2670 kg/m³ for the upper crust, from the surface down to 20 km depth, and 2900 kg/m³ for the lower crust, from 20 to 35 km depth. The densities ascribed to the subcontinental lithospheric mantle are from Poudjom-Djomani *et al.* (2001) estimates. According to the geochronological ages of the main units (Archean cratons), we use the mantle density estimate of 3310 kg/m³.

The gravity modelling begins with three polygons. The first polygon represents the upper crust, with its top defined as the surface topography, its bottom at 20 km, and a normal density of 2670 kg/m³. The second polygon represents the lower crust with a normal density of 2900 kg/m³ and depth limits between 20 and 35 km, the average crust-mantle boundary at sea level. The third polygon represents the variations in the crustal thickness defined between 35 km and the Moho depth shown in Fig. 4(a), also with a normal density of 2900 kg/m³. We then partition these polygons into distinct lateral sections and change their densities by small amounts until the calculated gravity fits the observed long-wavelength residual gravity anomalies.

Profiles B-B’ and C-C’ of the gravity models are shown in Figs. 7 and 8, respectively, and Figs. S4 and S5 (supplementary material) show the results of the gravity modelling for profiles A-A’ and D-D’. In Figs. 7 and 8, panel (a) shows the topography, the Moho depth and the digitised MT resistivity section; (b) shows the residual Bouguer anomaly, the gravity due to the Moho, as calculated in Fig. 4(b), and the calculated gravity derived from the crustal model presented in (c). The density contrast assumed for the crust in (c) is the same from Moho depth to the surface topography. The segment of each modelled gravity profile, which crosses the gravity gradient, is represented by a grey zone, and the granites closer to it are shown in white triangles. In Fig. 6(b), the same area is shown by a purple dashed line over the white solid profile line.

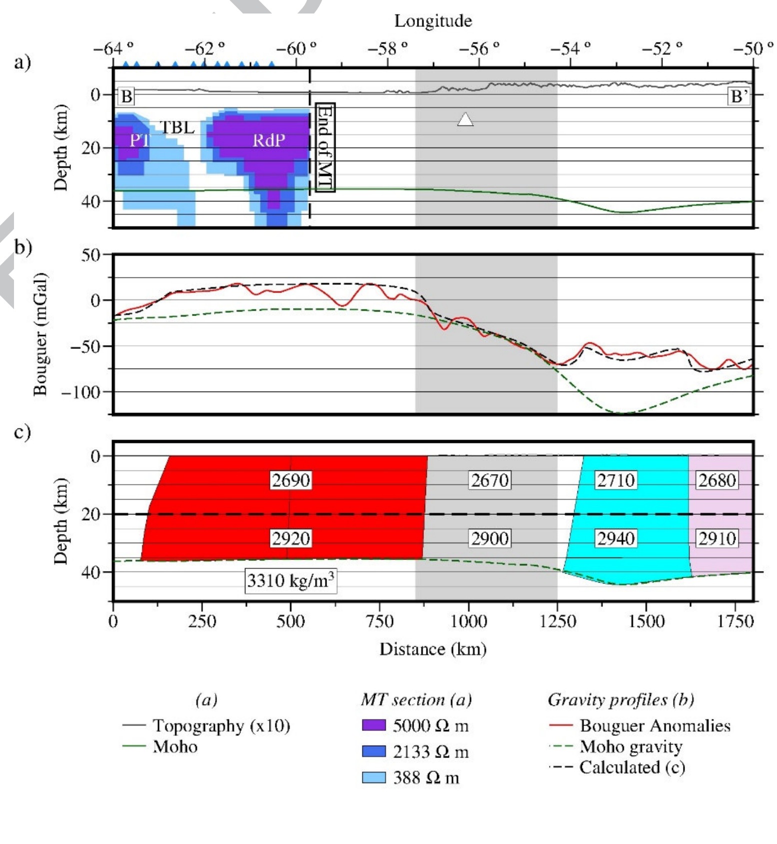

Figure 7 – Profile B-B', after removing the sediments and basalts gravity effects. The light grey shade marks the suture zone and the white triangle is the closest granite, as shown in Fig. 6(b). a) 10x vertical exaggeration topography (grey line), crustal thickness from Fig. 4(a) (green line); vertical axis is positive downwards. MT resistivity section digitised from Peri *et al.* (2013) with TBL and PT interpreted by the authors as the Transbrasiliano lineament and the Pampia terrane, respectively, and RdP is their proposed Rio de la Plata craton. b) Observed residual Bouguer anomaly (red line), Moho gravity from Fig. 4(b) (dashed green line), calculated gravity (dashed black line). c) Gravity derived crustal model. Densities inside white boxes are in kg/m^3. The same density contrast was adopted for both the upper and lower crust.

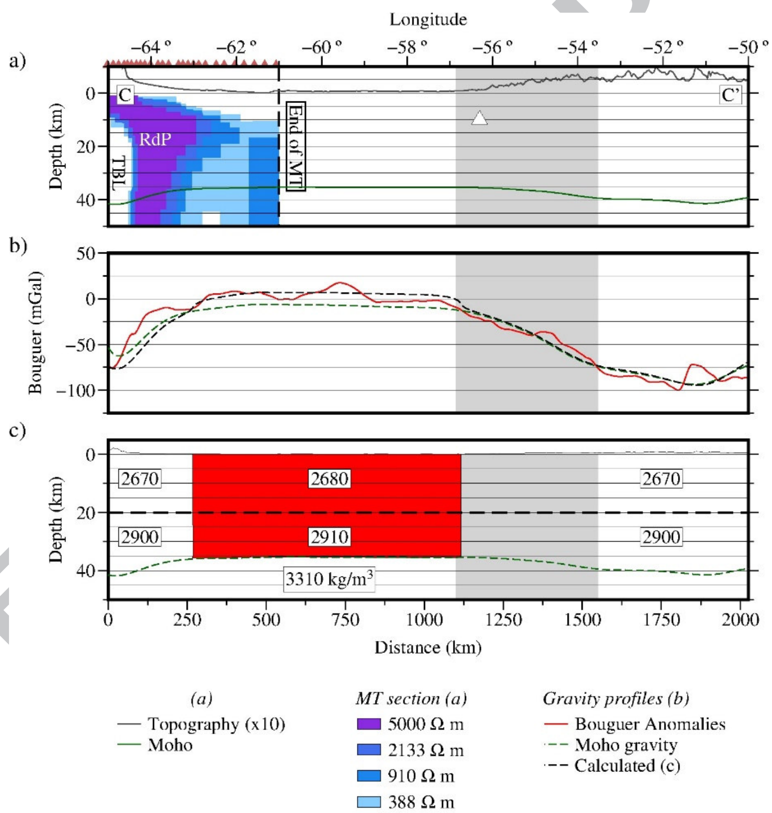

Figure 8 – Profile C-C'. Favetto *et al.* (2008) and Orozco *et al.* (2013) MT resistivity section was digitised and modified from Peri *et al.* (2013). See also Fig. 7 caption and legend.

"Insert Supplementary Figures S4 and S5 here"

4. Discussion

4.1 Interpretation of the gravity models

Profile B-B' starts at the circular gravity high to the north of the Chaco-Paraná basin and it coincides with a MT resistivity section (Peri *et al.*, 2013), as shown in Fig. 8(a). The amplitude of the residual gravity anomaly over the Chaco-Paraná basin is approximately 10 mGal. The profile crosses the gravity gradient and continues over the Paraná basin, reaching a minimum of -80 mGal. Overall, the gravity effect predicted solely by the Moho depth (Sec. 3.2, Fig. 4) does not fit the observed Bouguer gravity anomaly, as shown in Fig. 5(b) (dashed green vs. solid red). Also, a local gravity high is observed between longitudes 54° W and 51° W, superimposed to a regional or longer wavelength gravity low of -150 mGal.

The crusts of the Chaco-Paraná and the Paraná basins are distinct because they differ by at least 10 km in thickness, as shown in Fig. 8(a) (continuous green line). Yet, the gravity effect owing to this crustal thickness variation (Fig. 8(b), dashed green line) does not account for the observed gravity anomaly. According to the gravity modelling shown in Fig. 8(c), a density increase of 20 kg/m³ in the crust of the Chaco-Paraná basin is required to explain the observed gravity anomaly. The local gravity high over the central Paraná basin also predicts a density increase, very likely due to the emplacement of denser material during the Serra Geral volcanism. Mariani *et al.* (2013) modelled this accretion restricted to the lower crust and interpreted it as underplating, where basaltic melts are intruded as sills and also added to the base of the crust. Basalts may turn into gabbros at lower crust pressure condition, which often makes it difficult to be detected by seismological methods (An and Assumpção, 2006; Thybo and Artemieva, 2013). Using this model of underplating, a density increase of 210 kg/m^3 limited to the lowest 10 km of the crust explains the observed gravity anomaly. We propose for the Paraná basin an alternative density distribution instead, with a whole crust density increase of 40 kg/m³ (Fig. 8(c)). This second model is consistent with a recent magnetotelluric and geomagnetic deep sounding (GDS) study by Padilha *et al.*, (2015) in the Paraná basin, which detected a decrease in the bulk electrical resistivity in the crust and upper mantle.

Both gravity models predict mafic dykes intruding the crust during the Serra Geral flood basalt volcanism, affecting the Paraná basin in the Early Cretaceous, and adding magma to the base of the crust, thickening it.

In profile C-C', a density increase of 10 kg/m^3 was estimated for the entire crust in the Chaco-Paraná basin, resulting in a 2910 kg/m^3 lower and 2680 kg/m^3 upper crusts, whereas in the Paraná basin their densities are 2900 kg/m^3 and 2670 kg/m^3, respectively. Similar changes in crustal properties are also observed along profile A-A' and profile D-D' (Figs. S4 and S5 as supplementary material). These results indicate that the gravity gradient separates two crusts with distinct crustal thickness and composition.

4.2. The gravity gradient: a suture revealed

The gravity analysis carried out in the last section shows that the gravity gradient separates two crustal and lithospheric domains. The circular positive residual gravity anomalies to the west of the gradient (Fig. 6) are located in an area where crustal thickness is less than 35 km (Fig. 4(a). The gravity models (Figs. 7 and 8) show that in the Chaco-Paraná basin an entire crust density increase of 10 to 20 kg/m^3 is expected. Instead, in the Paraná basin, a thicker crust of more than 42 km is observed (Fig. 4(a)) and a normal density is predicted by the gravity modelling, except in areas intruded by the Serra Geral basalts.

S-wave seismic velocity models also show that the western side of the gradient is characterised by low velocity anomalies, as opposed to the high velocity anomalies in the Paraná basin to the east (Snoke and James, 1997; Feng *et al.*, 2007; Schaeffer and Lebedev, 2013; Rosa *et al.*, 2016). The velocity distribution on both sides of the suture spans the upper mantle, from 50 km depth down to 200 km, the base of the lithosphere. This lateral variation in seismic property is due to either distinct composition or thermal condition.

The area to the west of the gradient, comprising the Pantanal, the Paraguayan sector of the Chaco-Tarija and Chaco-Paraná basins, is overlain by Quaternary sedimentary deposits related to Andean tectonics (Ussami *et al.*, 1999; Chebli *et al.*, 1999; Kruck *et al.*, 2011), as shown in Fig. 1 and Fig. 3. These deposits cover a lowland plain of no more than 100 m of altitude. This area is also characterised by the absence of a major post-Paleozoic tectonism resulting in a flat relief and only a few basement outcrops (Russo *et al.*, 1986; Pezzi and Mozetic, 1989). On the eastern side of the gravity gradient, the Paraná basin is characterised by a higher topography, varying from ~300 m within the basin depocentre and parallel to the Paraná River, to ~700 m along its borders, where outcrops of every major sedimentary sequence are exposed. Moreover, the youngest sedimentation (Bauru group) in the Paraná basin is Late Cretaceous (Fig. 3 and Milani *et al.*, 1998). These geomorphological and geological observations are evidences that these crustal segments have undergone distinct tectonic evolution in spite of a common subsidence history during most of the Paleozoic to Early Mesozoic.

The stratigraphic records of the Chaco-Paraná and Paraná basins show that they have synchronously evolved during the Neopaleozoic and Mesozoic, right after the deglaciation of the Western Gondwana (Milani and Zalán, 1999). In the Early Cretaceous, however, after the Serra Geral flood volcanism (134.8 ± 1 Ma; Thiede and Vasconcelos, 2010) and the inception of the South Atlantic opening, the subsidence of these two intracontinental basins followed different histories. In the Paleocene, 350 m of marine facies sedimentary rocks, the Mariano Boedo Formation (Milani and Zalán, 1999), documents marine transgression over the Chaco-Paraná basin with no equivalent in the Paraná basin. And, from the Miocene on, the Chaco-Paraná basin is established as a distal foreland basin (Ramos, 1999), receiving a massive sedimentation from the Andes. Over the same period, the Paraná basin stratigraphic record, on the other hand, registers only the Bauru group, which was deposited in the Late Cretaceous. The subsidence in this period is related to thermal effects after the Serra Geral volcanism (Milani *et al.*, 1998). Crustal growth and uplift of the Paraná basin associated with the Serra Geral volcanism may be the main cause of its detachment from the Chaco-Paraná basin tectonic evolution.

The geological histories and the physical properties of the lithospheres of the Chaco-Paraná and Pantanal basins to the west and the Paraná basin to the east of the linear gravity gradient (Fig. 3) are distinct. This continental scale geophysical feature is hereafter referred to as the Western Paraná suture/shear zone and it marks the amalgamation of Archean to Paleoproterozoic cratonic lithospheres with the Paraná basin (and lithosphere) in Neoproterozoic to Cambrian times.

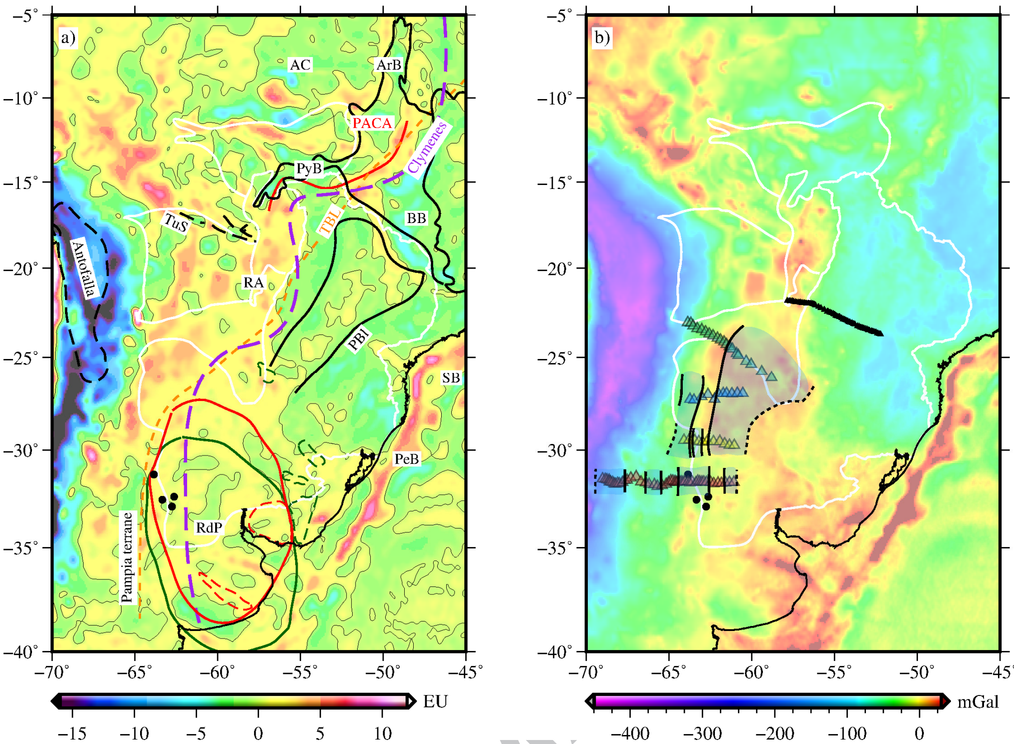

Figure 9 – a) Proposed main tectonic features of SW Gondwana by several authors overlaying the vertical derivative gravity map. References: PACA (**P**araguay **C**onductivity **A**nomaly, Bologna *et al.*, 2014) as red continuous line; Clymene Ocean in purple dashed line (Tohver *et al.*, 2012); PBl – Paranapanema block in black continuous line (Mantovani *et al.*, 2005); Rio de la Plata craton limits in continuous green (Oyhantçabal *et al.*, 2010) and red lines (Rapela *et al.*, 2011); São Francisco craton (SFC), Araguaia (ArB), Paraguay (PyB) and Brasília (BB) belts (Trompette, 1994); Transbrasiliano Lineament (TBL) (red dashed line adapted from Ramos *et al.*, 2010 and Daly *et al.*, 2014); TuS - Tucavaca syncline (Litherland and Bloomfield, 1981); black dots inside the Rio de la Plata craton are wells that reached the basement (Rapela *et al.*, 2011). b) Bouguer anomaly map. The coloured and black triangles are the MT stations as in Fig. 6. The blue shaded zones are the main electrical resistive units in the MT sections. See text for details.

4.3. Cratons to the west of the suture

We now present a discussion on each of the main tectonic units separated by the Western Paraná suture/shear zone. Fig. 9(a) summarises the tectonic units and lineaments already proposed by several authors in the context of SW Gondwana amalgamation. Fig. 9(b) is the residual Bouguer anomaly map together with the location of four MT profiles in Argentina and one MT profile in Brazil.

4.3.1. The Rio de la Plata craton

The map in Fig. 9(b) shows two positive gravity anomalies domains within the Chaco-Paraná basin, one to the south and other to the north of latitude 30° S. Moreover, to the south of this latitude, the vertical derivative gravity map Fig. 9(a) is dominated by several local and short wavelength negative anomalies, whereas in the northern domain the vertical derivative gravity map is smoother with only a few short wavelength negative anomalies. In both gravity maps, the latitude 30° S is the divide between the northern and southern gravity domains, suggesting that the basement beneath the Chaco-Paraná basin is composed of two tectonic units. The four MT profiles in Argentina shown in Fig. 9(b) also suggest this division, since the electrically resistive units mapped by the three northern MT profiles are laterally aligned whereas the MT profile along latitude 31.5° S (Favetto *et al.*, 2008 and Orozco *et al.*, 2013) has a lateral variation in the electrical resistivity which differs from the northern MT sections.

The southern segment of the Chaco-Paraná basin basement is the more detailed studied Rio de la Plata craton, a crust of Archean to Paleoproterozoic ages (Rapela *et al.*, 2007). Its exact limits however are still a matter of debate (Fig. 9(a)), as demonstrated in two geochronological and isotope geochemistry papers with distinct proposition of its limits (Oyhantçabal *et al.*, 2010 and Rapela *et al.*, 2011). Difficulties in determining the exact limits of the craton are due to the coverage by Quaternary sediments. Only a limited number of samples from boreholes and scattered rocks mainly at the continental margin were dated so far to constrain its limits. We correlate and define the limits of the Rio de la Plata craton with a gravity highs and negative vertical derivative anomalies to the south of 30° S, since they coincide with Paleoproterozoic age terranes dated by Rapela *et al.* (2007, 2011) and further south, along the Argentina continental margin, by Pangaro and Ramos (2012) using gravity and aeromagnetic data.

This offshore limit may be extended further south-eastwards where the same pattern of negative anomalies in the vertical derivative gravity map is observed (Fig. 9a).

Figure 10 shows the limits of the Rio de la Plata craton according to these gravity and gravity derivative maps. However, to the north-east, although the same gravity fabric continues, the Rio de la Plata craton could be limited at the Ibaré Shear Zone (ISZ, Fig. 10). This shear zone is located south of the Tacuarembó (granulites) terrane (Hartmann *et al*., 1999) and the juvenile São Gabriel magmatic arc (Babinski *et al*., 1996). Dating of the ophiolites that occur along ISZ, by Arena *et al*. (2016) through isotopic analysis of zircons, indicates an ocean closure in the Neoproterozoic, between 0.7 and 0.9 Ga. These terranes are located south of the gravity gradient (and W Paraná shear/suture zone).

The MT sections are roughly imaging two main resistive units juxtaposed, the Pampia terrane and the Rio de la Plata craton, as interpreted by their authors (see Favetto *et al.* (2015) for a compilation). Nevertheless, another fabric is observed in the MT section that imaged the lithosphere along the 31° S transect, as depicted in Fig. 9(b). The presence of an intermediate resistive unity could be explained by the formation of the Pampia terrane. According to Chernicoff *et al.* (2012), it began by the accretion in the Mesoproterozoic of a Greenville-type orogen to the western border of the Rio de la Plata craton. Part of this Greenville-type orogen would have rifted and later collided again with the Rio de la Plata craton, generating the complex resistive fabric at this sector. Moreover, the area defined by these authors for the Pampia terrane is coincident with a N-S alignment of negative anomalies in the vertical derivative gravity map and to an electrically resistive zone that extends over the three southern MT sections. Geophysically, these features do not continue north of latitude 30° S as shown by our gravity maps and by Favetto *et al.*'s (2015) MT study, since the western portion of the profile, where a resistive unity was expected, yielded a model with conductive lithosphere. Therefore, the proposition of a northern extension of the Pampia terrane needs further investigation. In Fig. 10, we follow the proposition of Ramos *et al.* (2010) of the continuation of the Pampia terrane towards the south Amazonian craton, but we mark the uncertain area to the north with a dashed contour.

4.3.2. The Rio Tebicuary craton

The gravity high in Fig. 9(b) and the homogeneous positive gravity fabric in the vertical derivative map in Fig 9(a) to the north of 30° S suggest the lithosphere to be an independent tectonic unit (Fig. 10) from the Rio de la Plata craton. This hypothesis finds support from geological and geophysical evidences other than gravity. Although less studied than the Rio Apa and Rio de la Plata cratons, basement rocks near the Tebicuary River, in the centre of the gravity high in southern Paraguay, were dated by Cordani *et al.* (2001) yielding concordant $^{207}Pb/^{206}Pb$ dates of 2023±12Ma, but no further sampling and dating has been carried out since then. Basement reworking is suggested by Ar-Ar, Rb-Sr and Sm-Nd dating with Brasiliano orogeny ages between 600 to 560 Ma. However, similar geophysical signatures observed in the neighbouring cratons such as high electrical resistivity (Favetto *et al.*, 2015) from MT soundings, positive gravity anomalies (this study) and thin (< 30 km) crust (Rosa *et al.*, 2016) allow us to classify this unit, in spite of restricted number of samples, as cratonic. This basement segment of the Chaco-Paraná basin is the Rio Tebicuary craton and its limits are shown in Fig. 10.

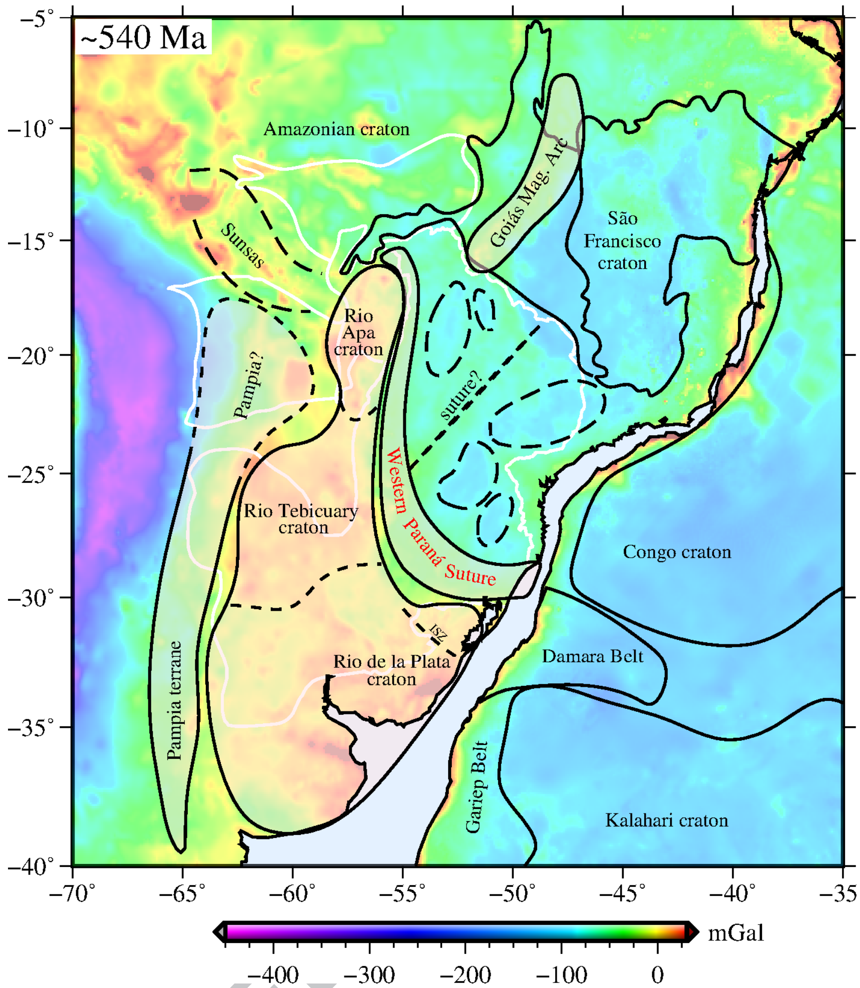

Figure 10 – Bouguer anomaly map of SW Gondwana with the South American plate rotated back to ~540 Ma to fit the African plate. For Africa, we use EGM08 gravity data. The new proposed tectonic units are in shaded red transparency (sutures and cratons to the west of the gravity gradient) and dashed black lines inside the Paraná basin (small terranes or cratonic blocks). The separation of the cratons to the west of the Western Paraná suture uses the gravity and vertical derivative gravity maps, which may not coincide exactly with the geological limit of the cratonic lithosphere. ISZ is the Ibaré Shear Zone, setting the north-eastern limit of the Rio de la Plata craton. See section 4.3.1 for detail. Congo and Kalahari cratons and Damara belt limits are from Foster *et al.* (2015). This digital gravity model and its vertical derivative are freely available upon request. The South America tectonic units herein discussed are shown superimposed to the geological map as supplementary material, Figure S6.

The three northern MT geoelectrical sections (Fig. 9(b)) imaged an electrically resistive lithosphere in the same region of the gravity high. This resistive lithosphere, although interpreted as being part of the Rio de la Plata craton, should now be revised if the gravity interpretation (Fig. 10), which separates the Rio Tebicuary from the Rio de la Plata cratons, is accepted. Likewise, a recent surface-wave tomography by Rosa *et al.* (2016) indicates that the northern portion of the Chaco-Paraná basin, thus coincident with the gravity high, is characterised by a much thinner crust (28 to 30 km) than the estimate in Section 3.2 (Fig. 4(a)). These authors also inferred a negative S-wave velocity perturbation in the mantle underneath the Chaco-Paraná basin, especially in this northern part suggesting the presence of a shallower asthenosphere.

4.3.3. The Rio Apa craton

In the north-western side of the Western Paraná suture/shear zone, another circular gravity high correlates, in its southern portion, with an exposed segment of the Rio Apa block and continues northward under the Pantanal basin (Fig. 9(b)). In the exposed segment of the Rio Apa block, Cordani *et al.* (2010), using U-Pb of zircons, obtained 1.7 to 1.9 Ga (Paleoproterozoic) ages and younger samples related to a Brasiliano orogeny overprint. Also, Sm-Nd T_{DM} model ages are between 1.9 and 2.5 Ga (Archean to Paleoproterozoic). The vertical derivative gravity map (Fig. 9(a)) also shows a positive anomaly without short wavelength gravity anomalies over the whole area, indicating that the Rio Apa block may cover a broader region (see Fig. 9(b)), encompassing the Pantanal basin basement and reaching the southern border of the Sunsás orogeny (Tassinari and Macambira, 1999). The vertical derivative map also reveals a series of small negative anomalies over the basement to the west of the Rio Apa craton. This is in accordance with the structural geology study in the Vallemi region (Paraguay, south Rio Apa craton) by Campanha *et al.* (2010), who concluded that this fragment of cratonic crust was affected by opposed vergence E-W compression. In the western border, the metamorphism and deformation is associated with eastward compression by the Pampia terrane, whereas in the eastern border it is the Western Paraná suture/shear zone. The MT study by Padilha *et al.* (2015) (see Fig. 9b for location) set up a 1200 km long profile extending from Rio Apa craton towards the Paraná basin. The geoelectrical section across the Rio Apa craton shows a typical electrical resistivity lithosphere section: high resistivity upper crust, moderate resistivity lower crust and again a more resistive upper mantle.

Both the gravity map and its vertical derivative also show that the Rio Apa craton is a segment of cratonic lithosphere independent from the Amazonian craton. The Rio Apa craton, likewise the two other cratonic units to the south has positive gravity anomaly and normal to thin crust (35 km), whereas the southern border of the accreted Amazonian craton is dominated by east-west trending and more negative gravity anomalies. The northern limit of the Rio Apa craton is under the Pantanal basin and the metasediments of the Paraguay fold/thrust belt.

4.3.4. Remarks on the nature and origin of the cratons

The three cratons to the west of the Western Paraná suture zone have a thinner and denser crust than the other cratons in Western Gondwana. The thickness of the crust in the Amazonian and the São Francisco cratons are between 40 and 45 km, as shown by Assumpção *et al.* (2013). These cratons have higher P- and S-wave velocities in the upper mantle. Likewise, Congo and Kalahari cratons in Africa have crustal thicknesses above 40 km, as shown by Pasyanos and Nyblade (2007). An extended gravity map in Fig. 10, with EGM2008 (Pavlis *et al.* 2008) Bouguer anomaly data for the African continent, shows negative gravity anomalies over the African cratons. The gravity anomalies of the Rio de la Plata, Rio Tebicuary and Rio Apa cratons are circular and positive, this leads to the following questions: where and how these ancient pieces of continental crusts originated? Rudnick (1995) reviewed some of the dilemmas and paradoxes still unresolved in explaining ancient continental crust generation, and it is beyond the scope of the present paper to discuss them. Basically, crustal growth occurs in two different tectonic settings, intraplate and in convergent margins. Within the context of the SW Gondwana construction, Paraná basin transformation into a large igneous province could be an example of intraplate growth of continental crust, whereas the accretion of the Pampia, Antofalla-Antofagasta terranes (Ramos, 2008) along the proto-Andean margin is an example of this process in a convergent margin. However, both examples are Phanerozoic and within the tenets of the present-day plate tectonics.

The issue of the formation of the Rio Apa, Rio Tebicuary and Rio de la Plata cratons in Archean or Paleoproterozoic times requires a deeper investigation, were they all formed in the same tectonic context, such as in a convergent margin? Modern example of such a process combining convergent margin tectonic setting together with "hot spot" processes were recently investigated along the Central America Pacific convergent margin. Using ambient noise seismic tomography, deep seismic crustal structures of thick oceanic crust in Costa Rica were imaged (Harmon and Rychert, 2015) which may indicate deep melt sills and enhanced production of felsic arc components, whereas in Nicaragua, where felsic arc is forming in a thinner crust, no evidence of the same sills was seismically detected. Hot spot process as proposed by Fyfe (1978) and others would predict a denser continental crust due to a more mafic crustal composition, as suggested by the positive gravity anomalies over the cratons of the present study. A thinner crust (~ 28 km, Rosa *et al.*, 2016) under the Chaco-Parana basin (or the Tebicuary craton) could be explained by a delamination process during the long lasting geological history, since a denser lower crust is gravitationally unstable (Bird, 1979).

4.4. The Paraná basin basement to the east of the suture

The Paraná basin crust to the east of the gradient has distinct regional gravity characteristics when compared to the cratonic areas to the west of the gradient, as detailed in Section 4.1.

Based on geochronological data, the Paraná basin basement was first associated with a cratonic nucleus due to rock samples in the central part of the basin with ~2.1 Ga K-Ar and ~1.0 Ga Rb-Sr ages (Cordani *et al.*, 1984). The cratonic Paranapanema block bordered by Neoproterozoic mobile belts was then proposed (Cordani *et al.*, 1984). Over a decade later, Milani (1997) and Milani and Ramos (1998) proposed that the Paraná basin basement should be constituted by several cratonic nuclei amalgamated during the Gondwana formation. This second model arose due to the Paleozoic Três Lagoas basalt (Mizusaki, 1989, *apud* Milani and Ramos, 1998). This basalt was sampled at the bottom of a well drilled in the centre of the previously proposed cratonic nucleus, suggesting the existence of a crustal/lithosphere discontinuity in the area.

Different geophysical works support both models. Mantovani *et al.* (2005) correlated a residual Bouguer gravity high in the Paraná basin centre to the Paranapanema block, whose limit was then given by the gravity gradient towards negative anomalies. These authors suggested a cratonic lithosphere underneath the Paraná basin based on the evidence of a thick crust and high seismic velocity anomalies estimated from previous seismological studies in the same area (Snoke and James, 1997; Assumpção *et al.*, 2002). Years later, Juliá *et al.* (2008), using a network of seismic stations in the northern portion of the Paraná basin, suggested that mafic underplating occurred preferentially alongside the suture zones proposed by Milani (1997) and Milani e Ramos (1998), thus supporting the idea of a mosaic of fragmented cratonic pieces and terranes composing the Paraná lithosphere.

Gravity data is useful and less ambiguous in mapping lateral variation of density distribution within the crust. However, estimating the vertical distribution is highly dependent on complementary geophysical data such as Moho depth estimates. The new gravity map and recent electromagnetic induction studies (Padilha *et al.*, 2015) allow us to further speculate about the Paraná basin basement. The short-wavelength gravity anomalies shown in the gravity map (Fig. 6) suggest that the Paraná basin crust is composed of small cratonic blocks and/or terranes (dashed lines in Fig. 10). In this case, the local NE-SW trending gravity high may indicate a Proterozoic suture/Paleozoic rift zone from where a major basalt outflow occurred. A deep well drilled near the Paraná river and within the basin depocentre (Três Lagoas city) has sampled a Late Ordovician basalt (Milani and Ramos, 1998) which may be a proxy of an extension along this suture during the Paleozoic. This NE-trending suture/rift zone separates the Paraná basement into eastern and western provinces (Figs. 9(a) and (b)). The existence of this suture or lithosphere discontinuity finds support from Padilha *et al.* (2015) electromagnetic induction study, since in their work a three-dimensional **G**eomagnetic **D**eep **S**ounding (GDS) inversion has mapped a crustal scale electrically conductive anomaly along the same NE direction. Geophysical evidence of a suture is consistent with the basin stratigraphy. The thickest sediment and basalt deposits (Fig. 4) correlate with this NE-trending high electrical conductive crust.

The Paraná basin lithosphere is separated from the São Francisco and Amazonian cratons by two electrically mapped suture zones (Bologna *et al.*, 2011 and Bologna *et al.*, 2014).

4.5. Age and nature of the Western Paraná suture/shear zone

The geological evidence of the Western Paraná suture is the presence of Neoproterozoic to Early Cambrian age granites (see Table 1) alongside the gravity gradient (Fig. 6). The granites to the east of the Pantanal basin (B1 to B4, Godoy *et al.*, 2010) and related to the Dom Feliciano belt (C3 and C4; Sartori and Kawashita, 1985, Phillip and Machado, 2005) are described as syntectonic and having calc-alkaline composition. The granites C1 and C2 (Wiens, 1986; Cubas *et al.*, 1998), which are less studied occur to the west of the suture along an exposed segment of the Rio Tebicuary cratonic basement. The width of the gravity gradient at this latitude (22° S) coincides with the region of sediments and basalts coverage (Fig. 3) therefore we cannot rule out the existence of granites associated with the same shear zone now concealed by the Paraná basin younger rocks. These granites are not only the geological evidence, but they provide important constraints on the age and nature of this suture. An attachment of the Rio de La Plata craton to the Paraná basin basement in the Neoproterozoic was until now an open question (Kröner and Cordani, 2003; Mantovani *et al.*, 2005) that seems to be resolved by the Western Paraná suture/shear zone. Suture zones marked by gravity gradients and lateral changes in geophysical properties (density, electrical resistivity and seismic velocities) are also observed across sutures between the São Francisco craton and the Paraná basin (Lesquer *et al.*, 1981, Bologna *et al.*, 2011) and the São Francisco craton - Goiás magmatic arc and the Amazonian craton (Ussami and Molina, 1999; Soares *et al.*, 2006). The Western Paraná suture is the largest lateral variation in the gravity anomaly and presents a major change in the physical properties of the lithosphere within the South American plate. The Western Paraná suture is not restricted to the continental area. It extends into the southeast Brazilian continental margin where it controls the distribution of the basins and its direction coincides with the Florianópolis Fracture Zone (Contreras *et al.*, 2010), a lineament that separates the Pelotas basin from the Santos basin. No extension of the Western Paraná suture appears in the African side (Fig. 10). A possible candidate, the Damara belt, is located to the south of the Western-Paraná suture/shear zone, as already mentioned in Section 4.3.4. Besides, the African cratons present negative gravity anomalies whereas the Rio de la Plata, Rio Tebicuary and Rio Apa cratons have positive Bouguer anomalies suggesting distinct crustal and lithosphere structure, therefore, distinct genesis and/or evolution.

4.6. Final Amalgamation of SW Gondwana

Geophysical data helped us to define a new element related to the SW Gondwana amalgamation history, the Western Paraná suture/shear zone. Two observations are straightforward. First, the continuation of the Transbrasiliano lineament (TBL) into Argentina and its connection with the Pampean belt (Ramos *et al.*, 2010) needs revision. Second, this Brasiliano tectonic feature does not cross the Paraná basin basement along the NE-SW direction within the western of the basin as envisaged by many authors (Cordani *et al.*, 2000, 2003; Ramos *et al.*, 2010). From its trace over the Goiás magmatic arc it may continue towards the southern border of the Amazonian craton, following the strong geoelectrical conductor PACA (Bologna *et al.*, 2014) and the magnetic lineaments mapped by Curto *et al.* (2014). These authors suggested that these lineaments reactivated during the Paleozoic and Mesozoic and contributed to the Paraná basin subsidence at that latitude. Their study is limited to 55° W in longitude and to the north of 17° S and only a single major fault (Serra Negra lineament) follows the N30°E direction, which coincides with the TBL trace whereas the majority of fault zones are sub-parallel (N60°E) to the Paraguay belt at the southern border of the Amazonian craton.

The Clymene Ocean proposed by Trindade *et al.* (2006) coincides with the trace of the TBL as proposed by Ramos *et al.* (2010) towards the Pampean belt in Argentina where Neoproterozoic granites, ophiolites and carbonate rocks are found. Tohver and Trindade (2014) suggest that the Neoproterozoic-Cambrian granites (Godoy *et al.*, 2010) are the proxies of a subduction of an oceanic plate in Cambrian times west of the Paraná basin (Fig. 10). From our study, these granites are the geological evidence of the Western Paraná suture/shear zone. This tectonic feature continues to the south-eastern Brazilian continental margin. In the light of the results shown in Fig. 10, the location of the Clymene Ocean closure ought to be revised, one possibility is the Paraguay belt connecting with the Pampean belt via the western border of the Rio Apa craton. The Rio Apa, Rio Tebicuary and Rio de la Plata cratonic masses were close to the proto-margin of the SW Gondwana continent. A low topography condition prevailed on and around these cratons. Thus, a shallow sea condition may have allowed the deposition of marine facies sediments and the carbonatic rocks of the Puncoviscana trough (Jezek *et al.*, 1985), the Corumbá Formation (Boggiani, 1998) over the Rio Apa craton and the Arroyo del Soldado Group (Gaucher *et al.*, 2003) over the Rio de la Plata craton in Uruguay. On the other hand, the carbonates of the Serra Azul Formation in the northern Paraguay belt developed at the edge of the Amazonian craton as part of a carbonatic platform deposited at the continental margin. According to Figueiredo and Babinski (2010), the carbonates of the northern Paraguay belt are distinct from its southern counterpart (Corumbá Fm and Arroyo del Soldado Group) as previously suggested by Boggiani (1998) based on C isotope and stratigraphical studies.

The location of the Western Paraná suture/shear zone and its age of closure are consistent with an east-west compression within the SW Gondwana, thus approximately coincident with the Pampean orogeny located at the western border of the cratons in Early Cambrian times. Almost 40 Myr separate the age of the Western Paraná suture/shear zone related granites from the anorogenic and younger granites related to the Paraguay fold/thrust belts (A1 - São Vicente, A2-Lajinha and A3-Araguainha in Table 1). One could speculate whether the final closure of the SW Gondwana was a two-phase process. The first one would be along the W Paraná suture and the Pampean belt as a result of an east-west compression. The second phase being the collage of the Amazonian craton and the formation of the Paraguay fold/thrust belt at the continental margin of this plate, closing the Clymene Ocean.

Alternatively, the final closure would be seen as a diachronous process whilst the Goiás-Pharusian ocean was closing (Pimentel and Fuck, 1992) at 580-600 Ma and the sea (Clymene?) between the southern Amazonian craton and the remaining masses, including the western edge of the Goiás magmatic arc, was still open. The final closure of the Clymene sea/ocean and the amalgamation of the SW Gondwana would take place with the formation of the Paraguay belt thrusting and deformation at 544 Ma as proposed by McGee *et al.* (2015). In this scenario, a rotation of the southern land masses (São Francisco craton, magmatic arcs, Paraná basin plate) could be accommodated along the Western Paraná suture/shear zone and generating compressional stresses against the southern Amazonian craton. The syntectonic granites (Godoy *et al.*, 2010) would be the proxies of this alternative process.

5. **Conclusions**

We elaborate a new gravity map of the intracontinental Paraná, Chaco-Paraná, Chaco-Tarija, Pantanal and Parecis basins using a gravity model available for the South American plate and open source terrestrial gravity data from Argentina, especially over the Chaco-Paraná basin. The analysis of the gravity maps and the gravity modelling of the crust, integrating other geophysical and geological information, allow us to propose: i) the Western Paraná suture/shear zone, separating the Paraná basin to the east from the Chaco-Paraná, Chaco-Tarija and Pantanal basins to the west; ii) the Rio Tebicuary craton, a new tectonic unit of Paleoproterozoic age basement concealed by the Chaco-Paraná basin, also imaged by magnetotelluric and seismological studies; iii) the west and east limits of the Rio Apa, Rio Tebicuary and Rio de la Plata cratons, along the Pampean belt and the Western Paraná suture zone, respectively.

Acknowledgments

This project was sponsored in Brazil by CAPES-MINCYT (project 234/13), FAPESP Thematic Projects 09/50493-8 and 12/06082-6, and in Argentina by MINCYT-CAPES (project BR/12/03). GND is sponsored by CAPES PhD scholarship, NU by CNPq grant (306284/2011-1), CAMC by FAPESP PhD scholarship (09/18511-6).

References

Amante, C.B. and Eakins, W., **2008**. ETOPO1 1 Arc-Minute Global Relief Model: Procedures, Data Sources and Analysis. NOAA Technical Memorandum NESDIS NGDC-24. National Geophysical Data Center, NOAA. doi: 10.7289/V5C8276M

An, M. and Assumpção, M., **2006**. Crustal and upper mantle structure in the intracratonic Paraná Basin, SE Brazil, from surface wave dispersion using genetic algorithms. *Journal of South American Earth Sciences*, v. 21, n. 3, pp. 173–184. doi: 10.1016/j.jsames.2006.03.001

Arena, K.R.; Hartmann, L.A.; Lana, Cristiano., **2016**. Evolution of Neoproterozoic ophiolites from the southern Brasiliano Orogen revealed by zircon U-Pb-Hf isotopes and geochemistry. *Precambrian Research*, v. 285, pp. 299-314. doi: 10.1016/j.precamres.2016.09.014

Assumpção, M.; James, D.; Snoke, A., **2002**. Crustal thicknesses in SE Brazilian Shield by receiver function analysis: Implications for isostatic compensation. *Journal of Geophysical Research*, v. 107, n. B1, pp. ESE 2-1–ESE 2-14. doi: 10.1029/2001JB000422.

Assumpção, M.; Feng, M.; Tassara, A.; Julià, J., **2013**. Models of crustal thickness for South America from seismic refraction, receiver functions and surface wave tomography. *Tectonophysics*, v. 609, pp. 82-96. doi: 10.1016/j.tecto.2012.11.014

Babinski, M.; Chemale Jr., F.; Hartmann, L.A.; Van Schmus, W.R.; da Silva, L.C., **1996**. Juvenile accretion at 750-700 Ma in southern Brazil. *Geology*, v. 25, n. 5, pp. 439-442. doi: 10.1130/0091-7613(1996)024<0439:JAAMIS>2.3.CO;2

Babinski, M.; Boggiani, P.C.; Trindade, R.I.F.; Fanning, C.M., **2013**. Detrital zircon ages and geochronological constraints on the Neoproterozoic Puga diamictites and associated BIFs in the southern Paraguay Belt, Brazil. *Gondwana Research*, v. 23, n. 3, pp. 988–997. doi: 10.1016/j.gr.2012.06.011

Bandeira, J.; McGee, B.; Nogueira, A.C.R.; Collins, A.S.; Ricardo Trindade, **2012**. Sedimentological and provenance response to Cambrian closure of the Clymene ocean: The upper Alto Paraguai Group, Paraguay belt, Brazil. *Gondwana Research*, v. 21, pp. 323-340. doi: 10.1016/j.gr.2011.04.006

Bird, P., **1979**. Continental delamination and the Colorado Plateau. *Journal of Geophysical Research*, v. 84, pp. 7561-7571. doi: 10.1029/JB084iB13p07561

Boggiani, P.C., **1998**. Análise estratigráfica da Bacia Corumbá (Neoproterozoico) - Mato Grosso do Sul. Ph.D. Thesis, Universidade de São Paulo, Sâo Paulo, Brazil.

Bologna, M.S.; Padilha, A.L.; Vitorello, Í.; Pádua, M.B, **2011**. Signatures of continental collisions and magmatic activity in central Brazil as indicated by a magnetotelluric profile across distinct tectonic provinces. *Precambrian Research*, v. 185, n. 1-2, pp. 55-64. doi: 10.1016/j.precamres.2010.12.003

Bologna, M.S.; Padilha, A.L.; Pádua, M.B.; Vitorello, Í.; Chamalaun, F.H., **2014**. Paraguay-Araguaia Belt Conductivity Anomaly: A fundamental tectonic boundary in South American Platform imaged by electromagnetic induction surveys. *Geochemistry, Geophysics, Geosystems*, v. 15, n. 3, pp. 509-515. doi: 10.1002/2013GC004970

Bomfim, E.P.; Braitenberg, C.; Molina, E.C., **2013**. Mutual evaluation of gravity models (EGM2008 and GOCE) and terrestrial data in Amazon basin, Brasil. *Geophysical Journal International*, v. 195, pp. 870–882. doi: 10.1093/gji/ggt283

Bruinsma, S.L.; Förste, C.; Abrikosov, O.; Marty, J.-C.; Rio, M.-H.; Mulet, S.; Bonvalot, S., **2013**. The new ESA satellite-only gravity field model via the direct approach. *Geophysical Research Letters*, v. 40, n. 14, pp. 3607-3612, doi: 10.1002/grl.50716

Campanha, G.A.daC.; Warren, L.; Boggiani, P.C.; Grohmann, C.H.; Cáceres, A.A., **2010**. Structural analysis of the Itapucumí Group in the Vallemí region, northern Paraguay: Evidence of a new Brasiliano/Pan-African mobile belt. *Journal of South American Earth Sciences*, v. 30, n. 1, pp. 1-11. doi: 10.1016/j.jsames.2010.04.001

Casquet, C.; Rapela, C.W.; Pankhurst, R.J.; Baldo, E.G.; Galindo, C.; Fanning, C.M.; Dahlquist, J.A.; Saavedra, J., **2012**. A history of Proterozoic terranes in southern South America: From Rodinia to Gondwana. *Geoscience Frontiers*, v. 3(2), pp. 137-145. doi: 10.1016/j.gsf.2011.11.004

Chaves, C.A.M. and Ussami, N., **2013**. Modeling 3-D density distribution in the mantle from inversion of geoid anomalies: Application to the Yellowstone Province, *Journal of Geophysical Research: Solid Earth*, v. 118, n. 12, pp. 6328–6351. doi: 10.1002/2013JB010168

Chebli, G.A.; Mozetic, M.E.; Rossello, E.A.; Buhler, M., **1999**. Cuencas sedimentarias de la Llanura Chacopampeana. In: Camino, R. (ed), *Geologia Argentina*. Argentina, Buenos Aires: SEGEMAR. pp. 627-644.

Chernicoff, C.J.; Zappettini, E.O.; Santos, J.O.S.; Godeas, M.C.; Belousova, E.; McNaughton, N.J., **2012**. Identification and isotopic studies of early Cambrian magmatism (El Carancho Igneous Complex) at the boundary between Pampia terrane and the Río de la Plata craton, La Pampa province, Argentina. *Gondwana Research*, v. 21, pp. 378-393. doi:10.1016/j.gr.2011.04.007

Chulick, G.S.; Detweiler, S.; Mooney, W.D., **2013**. Seismic structure of the crust and uppermost mantle of South America and surrounding oceanic basins. *Journal of South American Earth Sciences*, v. 42, pp. 260-276. doi: 10.1016/j.jsames.2012.06.002

Contreras, J.; Zühlke, R.; Bowman, S.; Bechstädt, T., **2010**. Seismic stratigraphy and subsidence analysis of the southern Brazilian margin (Campos, Santos and Pelotas basins). *Marine and Petroleum Geology*, v. 27, n. 9, pp. 1952-1980. doi: 10.1016/j.marpetgeo.2010.06.007

Cordani, U.G.; Brito Neves, B.B.; Fuck, R.A.; Porto, R.; Thomaz FIlho, A.; Cunha, F.M.B. da, **1984**. Estudo preliminar de integração do Pré-Cambriano com os eventos tectônicos das bacias sedimentares brasileiras. PETROBRAS, Cenpes, Sintep III, Série Ciência-Técnica-Petróleo, v. 15, pp. 1-70.

Cordani, U.G.; Sato, K.; Teixeira, W.; Tassinari, C.C.G.; Basei, M.A.S., **2000**. Crustal evolution of the South American platform. In: Cordani, U.G., Milani, E.J., ThomazFilho, A., y Campos, D.A. (eds.), *Tectonic Evolution of South America*. 31st International Geological Congress, Rio de Janeiro, pp. 19–40.

Cordani, U.G.; Cubas, N.; Sato, K.; Nutman, A.P.; Gonzales, M.E.; Pressner, J.L.B., **2001**. Geochronological constraints for the evolution of the metamorphic complex near the Tebicuary River, Southern Precambrian Region of Paraguay. Extended abstract. In: *III Simposio Sudamericano de Geologia Isotopica*, Pucon, Chile, 9 p.

Cordani, U.G.; D'Agrella-Filho, M.S.; Brito-Neves, B.B.; Trindade, R.I.F., **2003**, Tearing up Rodinia: the Neoproterozoic palaeogeography of South American cratonic fragments. *Terra Nova*, v. 15, pp. 350-359. doi: 10.1046/j.1365-3121.2003

Cordani, U.G.; Teixeira, W.; Tassinari, C.C.G.; Coutinho, J.M.V.; Ruiz, A.R., **2010**. The Rio Apa Craton in Mato Grosso do Sul (Brazil) and northern Paraguay: Geochronological evolution, correlations and tectonic implications for Rodinia and Gondwana. *American Journal of Science*, v. 310, pp. 981-1023. doi: 10.2475/09.2010.09

Cubas, N., Garcete, A., Meinhold, K.D., Benitez, J.C., Figueredo, L., Gonzalez, M.E., Burgaht, K.P. and Höhndorf, A., **1998**. Mapa Geológico de la República del Paraguay – Escala 1: 100.000, Hoja Villa Florida, MOPC. Asunción, 71 p.

Curto, J.B.; Vidotti, R.M.; Fuck, R.A.; Blakely, R.J., **2014**. The tectonic evolution of the Transbrasiliano Lineament in northern Paraná Basin, Brazil, as inferred from aeromagnetic data. *Journal of Geophysical Research*, v. 119, n. 3, pp. 1544-1562. doi: 10.1002/2013JB010593

Daly, M.C.; Andrade, V.; Barousse, C.A.; Costa, R.; McDowell, K.; Piggott, N.; Poole, A.J., **2014**. Brasiliano crustal structure and the tectonic setting of the Parnaíba basin of NE Brazil: Results of a deep seismic reflection profile. Tectonics, v. 33, n. 11, pp. 2102-2120. doi: 10.1002/2014TC003632

Dziewonski, A.M. and Anderson, D.L., **1981**. Preliminary reference earth model. *Physics of The Earth and Planetary Interiors*, v. 25, n. 4, pp. 297-356. doi: 10.1016/0031-9201(81)90046-7

ESA, **1999**. Reports for Mission Selection 'The Four Candidate Earth Explorer Core Missions', Gravity Field and Steady-State Ocean Circulation Mission. ESA Publication Division, ESA SP-1233(1).

Escayola, M.P.; Pimentel, M.M.; Armstrong, R., **2007**. Neoproterozoic backarc basin: Sensitive high-resolution ion microprobe U-Pb and Sm-Nd isotopic evidence from the Eastern Pampean Ranges, Argentina. *Geology*, v. 35, n. 6, pp. 495-498. doi: 10.1130/G23549A.1

Escayola, M.P.; van Staal, C.R.; Davis, W.J., **2011**. The age and tectonic setting of the Puncoviscana formation in northwestern Argentina: an accretionary complex related to early Cambrian closure of the Puncoviscana ocean and accretion of the Arequipa–Antofalla block. *Journal of South American Earth Sciences*, v. 32, n. 4, pp. 438-459. doi: 10.1016/j.jsames.2011.04.013

Favetto, A.; Pomposiello, C.; Luchi, M.G.L. de; Booker, J., **2008**. 2D Magnetotelluric interpretation of the crust electrical resistivity across the Pampean terrane – Río de la Plata suture, in central Argentina. *Tectonophysics*, v. 459, 1-4, pp. 54-65. doi: 10.1016/j.tecto.2007.11.071

Favetto, A.; Rocha, V.; Pomposiello, C.; García, R.; Barcelona, H., **2015**. A new limit for the NW Río de la Plata Craton Border at about 24ºS (Argentina) detected by Magnetotellurics. *Geologica Acta*, v. 13, 3, pp. 243-254. doi: 10.1344/GeologicaActa2015.13.3.6

Feng, M.; Lee, S. van der; Assumpção, M., **2007**. Upper mantle structure of South America from joint inversion of waveforms and fundamental mode group velocities of Rayleigh waves. *Journal of Geophysical Research*, v. 112, B04321. doi: 10.1029/2006JB004449

Figueiredo, M.F. and Babinski, M., **2010**. Paraguay Belt: The wind-up of Gondwana. Abstract presented at the Joint Assembly of the Americas, American Geophysical Union, Foz do Iguaçu, Brazil.

Foster, D.A.; Goscombe, B.D.; Newstead, B.; Mapani, B.; Mueller, P.A.; Gregory, L.C.; Muvangua, E., **2015**. U–Pb age and Lu–Hf isotopic data of detrital zircons from the Neoproterozoic Damara Sequence: Implications for Congo and Kalahari before Gondwana. *Gondwana Research*, v. 28, pp. 179-190. doi: 10.1016/j.gr.2014.04.011

Fyfe, W.S., **1978**. The evolution of the Earth´s crust: modern plate tectonics to ancient hot spot tectonics? *Chemical Geology*, v. 23, pp. 89-114. doi: 10.1016/0009-2541(78)90068-2

Gaucher, C.; Boggiani, P.C.; Sprechmann, P.; Sial, A.N.; Fairchild, T., **2003**. Integrated correlation of the Vendian to Cambrian Arroyo del Soldado and Corumbá Groups (Uruguay and Brazil): palaeogeographic, palaeoclimatic and palaeobiologic implications. *Precambrian Research*, v. 120, pp. 241-278. doi: 10.1016/S0301-9268(02)00140-7

Godoy, A.M.; Pinho, F.E.C.; Manzano, J.C.; Araújo, L.M.B.; Silva, J.A.; Figueiredo, M., **2010**. Estudos isotópicos das rochas granitóides neoproterozóicas da Faixa de Dobramento Paraguai. *Revista Brasileira de Geociências*, v. 40, n. 3, pp. 380-391.

Harmon, N. and Rychert, C.A., **2015**. Seismic imaging of deep crustal melt sills beneath Costa Rica suggests a method for the formation of the Archean continental crust. *Earth and Planetary Science Letters*, v. 430, pp. 140-148. doi: 10.1016/j.epsl.2015.07.062

Hartmann, L.A.; Leite, J.A.D.; McNaughton, N.J.; Santos, J.O.S., **1999**. Deepest exposed crust of Brazil-SHRIMP establishes three events. *Geology*, v. 27, n. 10, pp. 947-950. doi: 10.1130/0091-7613(1999)027<0947:DECOBS>2.3.CO;2

ICGEM, **2016**. International Centre for Global Earth Models. GFZ Helmholtz-Zentrum, Potsdam. http://icgem.gfz-potsdam.de/ICGEM/ (last access on 15/02/2016)

Introcaso, A., **1997**. *Gravimetría*. U.N.R. Editora, Rosario, 353 p.

Jezek, P.; Willner, A.P.; Aceñolaza, F.G.; Mille, H., **1985**. The Puncoviscana trough – a large basin of Late Precambrian to Early Cambrian age on the Pacific edge of the Brazilian shield, *Geologische Rundschau*, v. 74, pp. 573-584. doi: 10.1007/BF01821213

Julià, J.; Assumpção, M.; Rocha, M.P., **2008**. Deep crustal structure of the Paraná Basin from receiver functions and Rayleigh-wave dispersion: Evidence for a fragmented cratonic root. *Journal of Geophysical Research*, v. 113, B08318. doi: 10.1029/2007JB005374

Kennett, B.L.N., **1991**. Seismic velocity gradients in the upper mantle. *Geophysical Research Letters*, v. 18, n. 6, pp. 1115-1118. doi: 10.1029/91GL01340

Kröner, A. and Cordanmi, U.G., **2003**. African, southern Indian and South American cratons were not part of the Rodinia supercontinent: evidence from field relationships and geochronology. *Tectonophysics*, v. 375, pp. 325–352. doi: 10.1016/S0040-1951(03)00344-5

Kruck, W.; Helms, F.; Geyh, M.A.; Suiano, J.M.; Marengo, H.G.; Pereya, F., **2011**. Late Pleistocene-Holocene History of Chaco-Pampa Sediments in Argentina and Paraguay. *Quaternary Science Journal*, v. 60(1), pp. 188–202. doi: 10.3285/eg.60.1.13

Lemoine, F.G. *et al.*, **1998**. The development of joint NASA GSFC and NIMA geopotential model EGM96. NASA Technical Paper NASA/TP-1998-206861, Goddard Space Flight Center, Greenbelt, EEUU.

Lesquer, A.; Almeida, F.F.M.; Davino, A.; Lachaud, J.C.; Maillard, P., **1981**. Signification structurale des anomalies gravimétriques de la partie sud du Craton de São Francisco (Brèsil). *Tectonophysics*, v. 76 pp. 273–293. doi: 10.1016/0040-1951(81)90101-3

Litherland, M. and Bloomfield, K., **1981**. The Proterozoic history of eastern Bolivia. *Precambrian Research*, v. 15, pp. 157-179.

Mantovani, M.S.M.; Quintas, M.C.L.; Shukowsky, W.; Brito Neves, B.B., **2005**. Delimitation of the Paranapanema Proterozoic Block: A Geophysical Contribution. *Episodes*, v. 28, n. 1, p. 18-22.

Mariani, P.; Braitenberg, C.; Ussami, N., **2013**. Explaining the thick crust in Paraná basin, Brazil, with satellite GOCE gravity observations. *Journal of South American Earth Sciences*, v. 45, pp. 209-233, 2013. doi: 10.1016/j.jsames.2013.03.008

Marques, L.S.; Nardy, A.J.R.; Pinese, P.P.P.; Raposo, M.I.B., **1984**. Correlação entre densidade e equimismo dos principais litotipos vulcânicos da Bacio do Paraná. In: *33rd Congresso Brasileiro de Geologia*, Rio de Janeiro, Brazil, p. 253.

Martinec, Z., **1994**. The density contrast at the Mohorovičić discontinuity. *Geophysical Journal International*, v. 117, n. 2, pp. 539-544. doi: 10.1111/j.1365-246X.1994.tb03950.x

McGee, B.; Collins, A.S.; Trindade, R.I.F.; Jourdan, F., **2015**. Investigating mid-Ediacaran glaciations and final Gondwana amalgamation using coupled sedimentology and 40Ar/39Ar detrital muscovite provenance from the Paraguay belt, Brazil, *Sedimentology*, v. 62, pp. 130-154. doi: 10.1111/sed.12143

Melfi, A.J.; Piccirillo, E.M.; Nardy, A.J.R., **1988**. Geological and magmatic aspects of the Paraná basin an introduction. In: Piccirillo, E.M.; Melfi, A.J. (eds), *The Mesozoic Flood Volcanism of the Paraná Basin: Petrogenetic and Geophysical Aspects*. São Paulo, Brazil. Universidade de São Paulo, Instituto Astronômico e Geofísico, 600 p.

Milani, E.J., **1997**. Evolução tectono-estratigráfica da Bacia do Paraná e seu relacionamento com a geodinâmica fanerozóica do Gondwana Sul-ocidental. Ph.D thesis, Universidade Federal do Rio Grande do Sul, Porto Alegre, Brazil, 2v, 255 p.

Milani, E.J. and Ramos, V., **1998**. Orogenias paleozoicas no domínio sul-ocidental do Gondwana e os ciclos de subsidência da Bacia do Paraná. *Revista Brasileira de Geociências*, v. 28, n. 4, pp. 473-484.

Milani, E.J.; Faccini, U.F.; Scherer, C.M.; Araújo, L.M.; Cupertino, J.A., **1998**. Sequences and stratigraphic hierarchy of the Paraná Basin (Ordovician to Cretaceous), southern Brazil. Boletim IG USP, Série Científica, n. 29.

Milani, E.J. and Zalán, P.V., **1999**. An outline of the geology and petroleum systems of the Paleozoic interior basins of South America. Episodes, v. 22, n. 3, pp. 199-205.

Molina, E.C.; Ussami, N.; Sá, N.C. de; Blitzkow, D., **1989**. Interpretação dos dados gravimétricos da parte norte da bacia do Paraná. *Revista Brasileira de Geociências*, v. 19(2), pp. 187-196.

Morelli, C. *et al.*, **1972**. The International Gravity Standardization Net 1971. IUGG, International Association of Geodesy, Special Publication, n. 4.

Moritz, H., **1980**. *Advanced physical geodesy*. Karlsruhe: Wichmann, 500 p.

Moritz, H., **1984**. Geodetic reference system 1980. *Bulletin Géodésique*, v. 58, n. 3, pp. 388-398.

Nagy, D.; Papp, G.; Benedek, J., **2000**. The gravitational potential and its derivatives for the prism. *Journal of Geodesy*, v. 74, n. 7, pp. 552-560. doi: 10.1007/s001900000116

Orozco, L.A.; Favetto, A.; Pomposiello, C.; Rossello, E.; Booker, J., **2013**. Crustal deformation of the Andean foreland at 31° 30′S (Argentina) constrained by magnetotelluric survey. *Tectonophysics*, v. 582, pp. 126-139. doi: 10.1016/j.tecto.2012.09.030

Oyhantçabal, P.; Siegesmund, S.; Wemmer, K., **2010**. The Río de la Plata Craton: a review of units, boundaries, ages and isotopic signature. *International Journal of Earth Sciences*, v. 100, 2-3, pp. 201-220. doi: 10.1007/s00531-010-0580-8

Padilha, A.L.; Vitorello, Í.; Antunes, C.A.; Pádua, M.B., **2015**. Imaging three-dimensional crustal conductivity structures reflecting continental flood basalt effects hidden beneath thick intracratonic sedimentary basin. *Journal of Geophysical Research: Solid Earth*, v. 120, pp. 4702-4719. doi: 10.1002/2014JB011657

Pangaro, F. and Ramos, V.A., **2012**. Paleozoic crustal blocks of onshore and offshore central Argentina: New pieces of the southwestern Gondwana collage and their role in the accretion of Patagonia and the evolution of Mesozoic south Atlantic sedimentary basins. *Marine and Petroleum Geology*, v. 37, pp. 162-183. doi: 10.1016/j.marpetgeo.2012.05.010

Pasyanos, M.E.; Nyblade, A.A., **2007**. A top to bottom lithospheric study of Africa and Arabia. *Tectonophysics*, v. 444, n.1-4, pp. 27-44. doi: 10.1016/j.tecto.2007.07.008

Pavlis, N.K.; Holmes, S.A.; Kenyon, S.C.; Factor, J.K., **2012**. The development and evaluation of the Earth Gravitational Model 2008 (EGM2008). *Journal of Geophysical Research*, v. 117, B04406. doi: 10.1029/2011JB008916

Peri, V.G.; Pomposiello, M.C.; Favetto, A.; Barcelona, H.; Rossello, E.A., **2013**. Magnetotelluric evidence of the boundary between the Río de La Plata Craton and Pampean terrane (Chaco-Pampean Plain, Argentina): The extension of the Transbrasiliano Lineament. *Tectonophysics*, v. 608, pp. 685-699. doi: 10.1016/j.tecto.2013.08.012

Peri, V.G.; Barcelona, H. Pomposiello, C.; Favetto, A., **2015**. Magnetotelluric characterization through the Ambargasta-Sumampa Range: The connection between the northern and southern trace of the Río de La Plata Craton e Pampean Terrane tectonic boundary. *Journal of South American Earth Sciences*, v. 59, pp. 1-12.

Pezzi, E.E. and Mozetic, M.E., **1989**. Cuencas Sedimentarias de la Región Chacoparanense. In: Chebli, G.A.; Spalleti, L. (eds), *Cuencas Sedimentarias Argentinas*. Universidad Nacional de Tucumán, Argentina. Serie Correlación Geológica, n. 6, pp. 65-78.

Philipp, R.P. and Machado, R., **2005**. The Late Neoproterozoic granitoid magmatism of the Pelotas Batholith, southern Brazil. *Journal of South American Earth Sciences*, v. 19, pp. 461-478. doi: 10.1016/j.jsames.2005.06.010

Pimentel, M.M. and Fuck, R.A., **1992**. Neoproterozoic crustal accretion in central Brazil. *Geology*, v. 20, n. 4, pp. 375-379.

Poudjom Djomani, Y.H.; O'Reilly, S.Y.; Griffin, W.L.; Morgan, P., **2001**. The density structure of subcontinental lithosphere through time. *Earth and Planetary Science Letters*, v. 184, pp. 605-621. doi: 10.1016/S0012-821X(00)00362-9

Ramos, V.A., **1988**. Late Proterozoic-Early Paleozoic of South America. A collisional history. *Episodes*, 11, pp. 168-175.

Ramos, V.A., **1999**. Rasgos estructurales del territorio Argentino: Evolución tectónica de la Argentina. In: Caminos, R. (ed), *Geologia Argentina*. Buenos Aires, Republica Argentina. SEGEMAR, pp. 715-759.

Ramos, V.A., **2008**. The Basement of the Central Andes: The Arequipa and Related Terranes. *Annual Review of Earth and Planetary Sciences*, v. 36, pp. 289–324. doi: 10.1146/annurev.earth.36.031207.124304

Ramos, V.A.; Vujovich, G.; Martino, R.; Otamendi, J., **2010**. Pampia: A large cratonic block missing in the Rodinia supercontinent. *Journal of Geodynamics*, v. 50, 3-4, pp. 243-255. doi: 10.1016/j.jog.2010.01.019

Ramos, V.A.; Escayola, M.; Leal, P.; Pimentel, M.M.; Pimentel, Santos, J.O.S., **2015**. The late stages of the Pampean Orogeny, Córdoba (Argentina): Evidence of postcollisional Early Cambrian slab break-off magmatism. *Journal of South American Earth Sciences*. doi: 10.1016/j.jsames.2015.08.002

Rapalini, A.E.; Trindade, R.I.; Poiré, D.G., **2013**. The La Tinta pole revisited: Paleomagnetism of the Neoproterozoic Sierras Bayas Group (Argentina) and its implications for Gondwana and Rodinia. *Precambrian Research*, v. 224, pp. 51-70. doi: 10.1016/j.precamres.2012.09.007

Rapela, C.W.; Pankhurst, R.J.; Casquet, C.; Baldo, E.; Saavedra, J.; Galindo, C.; Fanning, C.M., **1998**. The Pampean Orogeny of the southern proto-Andes: Cambrian continental collision in the Sierras de Córdoba. *Geological Society, London, Special Publications*, v. 142, pp. 181-217. doi: 10.1144/GSL.SP.1998.142.01.10

Rapela, C.W.; Pankhurst, R.J.; Casquet, C.; Fanning, C.M.; Baldo, E.G.; González-Casado, J.M.; Galindo, C.; Dahlquist, J., **2007**. The Río de la Plata craton and the assembly of SW Gondwana. *Earth-Science Reviews*, v. 83, pp. 49-82. doi: 10.1016/j.earscirev.2007.03.004

Rapela, C.W.; Fanning, C.M.; Casquet, C.; Pankhurst, R.J.; Spalletti, L.; Poiré, D.; Baldo, E.G., **2011**. The Rio de la Plata craton and the adjoining Pan-African/brasiliano terranes: Their origins and incorporation into south-west Gondwana. *Gondwana Research*, v. 20, n. 4, pp. 673-690. doi: 10.1016/j.gr.2011.05.001

Rosa, M.L.; Collaço, B.; Assumpção, M.; Sabbione, N., Sanchez, G., **2016**. Thin crust beneath the Chaco-Paraná by surface-wave tomography. J. *South American Earth Sci*., v. 66, pp. 1-14. doi: 10.1016/j.jsames.2015.11.010

Rudnick, R.L., **1995**. Making continental crust. *Nature*, v. 378, pp. 571-578. doi: 10.1038/378571a0

Russo, A.; Archangelsky, S.; Andreis, R.R.; Cuerda, A., **1986**, Cuenca Chacoparanense. In: Archangelsky, S. (ed), *El sistema Carbonifero en la República Argentina*. Córdoba, Republica Argentina. Academia Nacional de Ciencias, pp. 197-212.

Sá, N.C. de., **2004**. O campo de gravidade, o geoide e a estrutura crustal na América do Sul: novas estratégias de representação. Habilitation thesis, Universidade de São Paulo, São Paulo, Brazil, 122 p.

Sartori, P.L.P. and Kawashita, K., **1985**. Petrologia e geocronologia do batólito granítico de Caçapava do Sul, RS. In: *Anais do II Simpósio Sul-brasileiro de Geologia*, Florianópolis/SC, Brazil, pp. 102-115.

Schaeffer, A.J. and Lebedev, S., **2013**. Global shear speed structure of the upper mantle and transition zone. *Geophysical Journal International*, v. 194, pp. 417-449. doi: 10.1093/gji/ggt095

Schenk, C.J.; Viger, R.J.; Anderson, C.P., **1999**. Maps showing geology, oil and gas fields, and geologic provinces of the South America region. USGS, open-file report 97-470D. https://catalog.data.gov/dataset/south-america-geologic-map-geo6ag (last access on 01/06/2015)

Smith, W.H.F. and Wessel, P., **1990**. Gridding with continuous curvature splines in tension. *Geophysics*, v. 55, n. 3, pp. 293-305. doi: 10.1190/1.1442837

Snoke, J.A. and James, D.E., **1997**. Lithospheric structure of the Chaco and Paraná basins of South America from surface-wave inversion. *Journal of Geophysical Research*, v. 102, n. B2, pp. 2939–2951. doi: 10.1029/96JB03180

Soares, J.E.; Berrocal, J.; Fuck, R.A.; Mooney, W.D.; Ventura, D.B.R., **2006**. Seismic characteristics of central Brazil crust and upper mantle: A deep seismic refraction study. *JGR: Solid Earth*, v. 111, n. B12302, pp. 1-31. doi: 10.1029/2005JB003769

Talwani, M.; Worzel, J.L.; Landisman, M., **1959**. Rapid gravity computations for two-dimensional bodies with application to the Mendocino submarine fracture zone. *Journal of Geophysical Research*, v. 64, n. 1, pp. 49-59. doi: 10.1029/JZ064i001p00049

Tassinari, C.C.G. and Macambira, M.J.B., **1999**. Geochronological provinces of the Amazonian Craton. *Episodes*, v. 22, n. 3, pp. 174-182.

Thiede, D.S. and Vasconcelos, P.M., **2010**. Paraná flood basalts: Rapid extrusion hypothesis confirmed by new $^{40}Ar/^{39}Ar$ results. Geology, v. 38, n. 8, pp. 747-750. doi: 10.1130/G30919.1

Thybo, H. and Artemieva, I.M., **2013**. Moho and magmatic underplating in continental lithosphere. *Tectonophysics*, v. 609, pp. 605-619. doi: 10.1016/j.tecto.2013.05.032

Tohver, E.; Trindade, R.I.F.; Solum, J.G.; Hall, C.M.; Riccomini, C.; Nogueira, A.C., **2010**. Closing the Clymene ocean and bending a Brasiliano belt: evidence for the Cambrian formation of Gondwana, southeast Amazon craton. *Geology*, v. 38, pp. 267-270. doi: 10.1130/G30510.1

Tohver, E.; Cawood, P.A.; Rossello, E.A.; Jourdan, F., **2012**. Closure of the Clymene Ocean and formation of West Gondwana in the Cambrian: Evidence from the Sierras Australes of the southernmost Rio de la Plata craton, Argentina. *Gondwana Research*, v. 21, 2-3, pp. 394-405. doi: 10.1016/j.gr.2011.04.001

Tohver, E. and Trindade, R.I.F., **2014**. Comment on “Was there an Ediacaran Clymene Ocean in central South America?” by U. G. Cordani and others. *American Journal of Science*, v. 314, pp. 805–813. doi: 10.2475/03.2014.03

Trindade, R.I.F.; D'Agrella-Filho, M.S.; Epof, I.; Brito Neves, B.B., **2006**. Paleomagnetism of Early Cambrian Itabaiana mafic dikes (NE Brazil) and the final assembly of Gondwana. *Earth and Planetary Science Letters*, v. 244, pp. 361–377. doi: 10.1016/j.epsl.2005.12.039

Trompette, R., **1994**. Geology of Western Gondwana (2000 – 500 Ma): Pan-African-Brasiliano aggregation of South America and Africa. Roterdam, Balkema, 350 p.

Ussami, N. and Molina, E.C., **1999**. Flexural modeling of the neoproterozoic Araguaia belt, central Brazil. Journal of South American Earth Sciences, v. 12, n. 1, pp.87–98. doi: 10.1016/S0895-9811(99)00007-3

Ussami, N.; Shiraiwa, S.; Dominguez, J.M.L., **1999**. Basement reactivation in a sub-Andean foreland flexural bulge: The Pantanal wetland, SW Brazil. *Tectonics*, v. 18, pp. 25-39. doi: 10.1029/1998TC900004

Wenzel, G., **1998**. Ultra-high degree geopotential models GPM98A, B and C to degree 1800. Preprint of a paper submitted to Bulletin of International Geoid Service, Milan (Italy), 13 p. http://www.ife.uni-hannover.de/

Wessel, P. and Smith, W.H.F., **1991**. Free software helps map and display data. Earth & Space Science News (EOS), v. 72, n. 41, pp. 441-446. doi: 10.1029/90EO00319

Wiens, F., **1986**. Zur lithostratigraphischen und strukturellen entwickelung des Rio Apa Hochlandes, Nordost Paraguay. Ph.D thesis, Clausthal University of Technology, Germany, 280 p.

Supplementary material

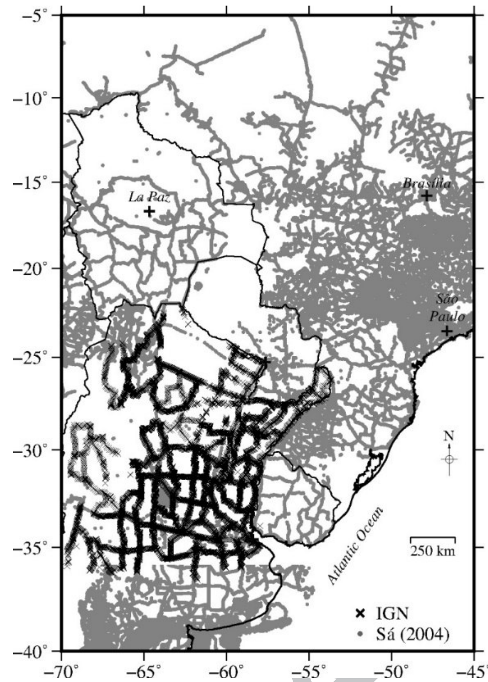

Figure S1 – Distribution of terrestrial gravity data used in the SAGM04 (Sá, 2004) (grey dots) and those from the IGN added to the present study (black crosses).

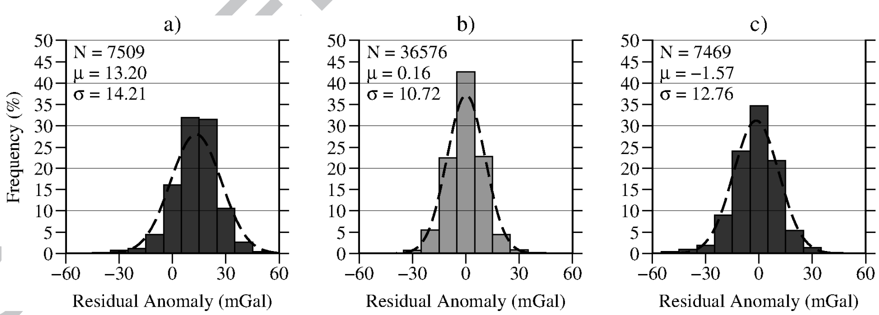

Figure S2 – Histograms of the differences between terrestrial and DIR_r5 satellite model Bouguer anomalies. a) IGN raw data; b) Brazilian data; c) IGN tied to the IGSN71 and cleaned (see also Fig. S3). N is the total number of stations, μ its mean value and σ the standard deviation. In order to refer all gravity observations to a common gravity reference system, we used a recent satellite-only gravity model named GO_CONS_GCF_2_DIR_R5 (Bruinsma *et al.*, 2013), hereafter referred to as DIR_r5. This model is publically available at the **I**nternational **C**entre for **G**lobal **E**arth **M**odels website (ICGEM, 2016). Differences between the IGN dataset and the DIR_r5 model were calculated and plotted on histogram (a). The histogram shows a Gaussian distribution with a mean value μ of 13.20 mGal, far from the expected zero value as shown for the Brazilian terrestrial data (b). Both the Brazilian data and the DIR_r5 model are tied to the 1971 **I**nternational **G**ravity **S**tandardization **N**et (IGSN71) (Morelli, 1972), whereas the IGN dataset is referenced to the local Miguelete gravity datum, thus requiring a -14.97 mGal correction in order to tie it to the IGSN71 (Introcaso, 1997).

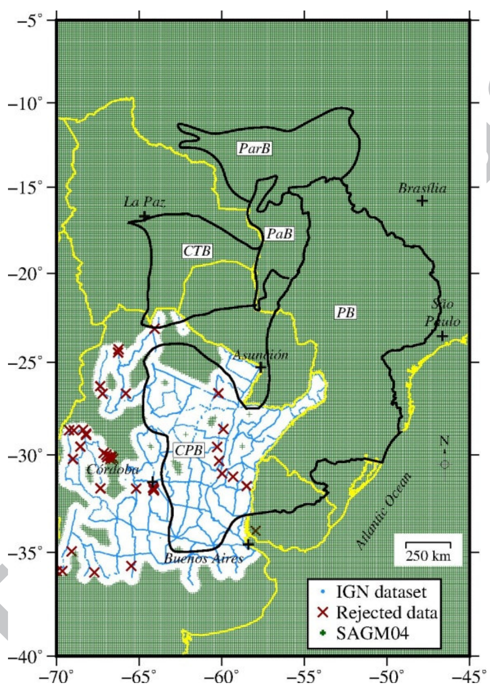

Figure S3 – Data used to compose the new gravity map. The IGN dataset is in blue dots with red crosses indicating the removed data. The SAGM04, a regular 5 min-arc grid, in green, completes the Bouguer anomaly map. The removal of outliers present in the IGN gravity database was the final step in the data editing. Each gravity data, the reference station, was compared with its seven closest ones, the targets. We estimated the difference between the mean Bouguer anomaly of the seven targets and the anomaly value of the reference station. We excluded the latter when this difference was larger than 2.5σ (standard deviation obtained from the residual histogram in Fig. S2(a)). Out of 7509 stations comprising the IGN dataset, 40 stations were discarded (histogram in Fig. 2(c)).

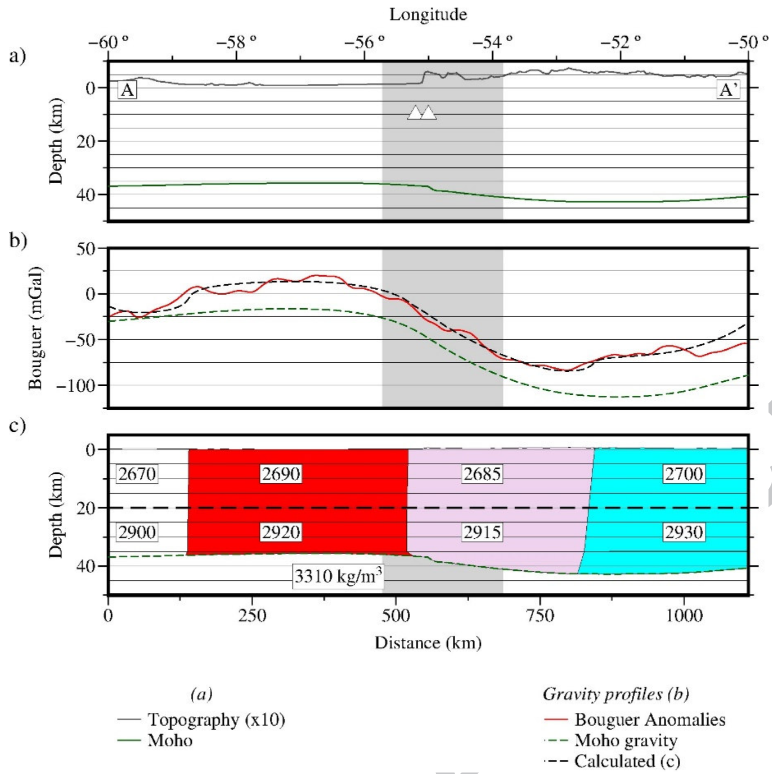

Figure S4 – Profile A-A', after sediments and basalts gravity effect removal. The light grey hachure is the region of the suture zone and the white triangle is the granite closer to the profile, as seen in Fig. 6(b). a) 10x vertical exaggeration topography (grey line), crustal thickness from Fig. 4(a) (green line); vertical axis is positive downwards. b) Observed residual Bouguer anomaly (red line), Moho gravity from Fig. 4(b) (dashed green line), calculated gravity (dashed black line). c) Gravity crustal model. Densities inside white boxes are in kg/m^3. The same density contrast was adopted for both the upper and lower crust.

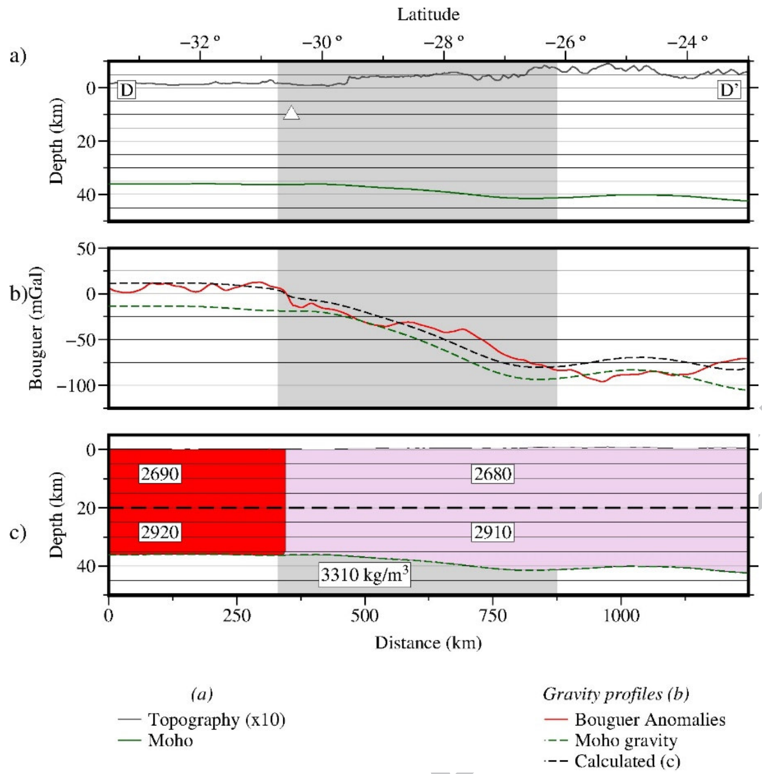

Figure S5 – Profile D-D', see Fig. S4 caption.

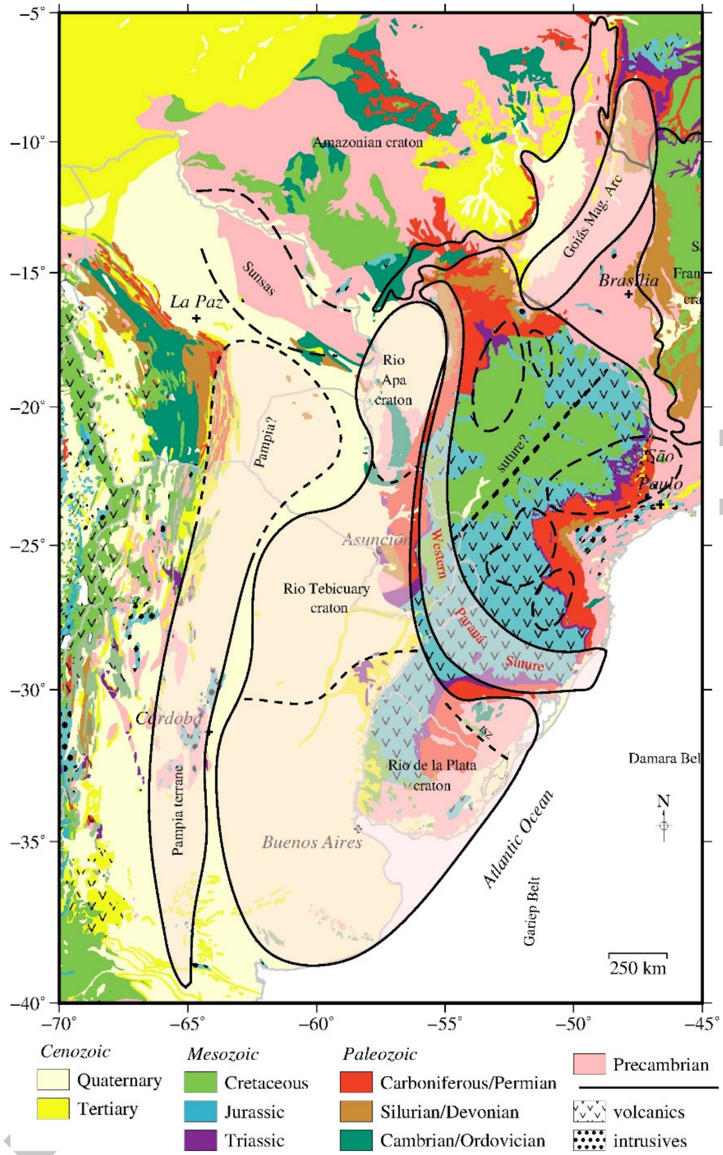

Figure S6 – Geological units discussed in this paper superimposed to the geological map adapted from the USGS (Schenk *et al.*, 1999).

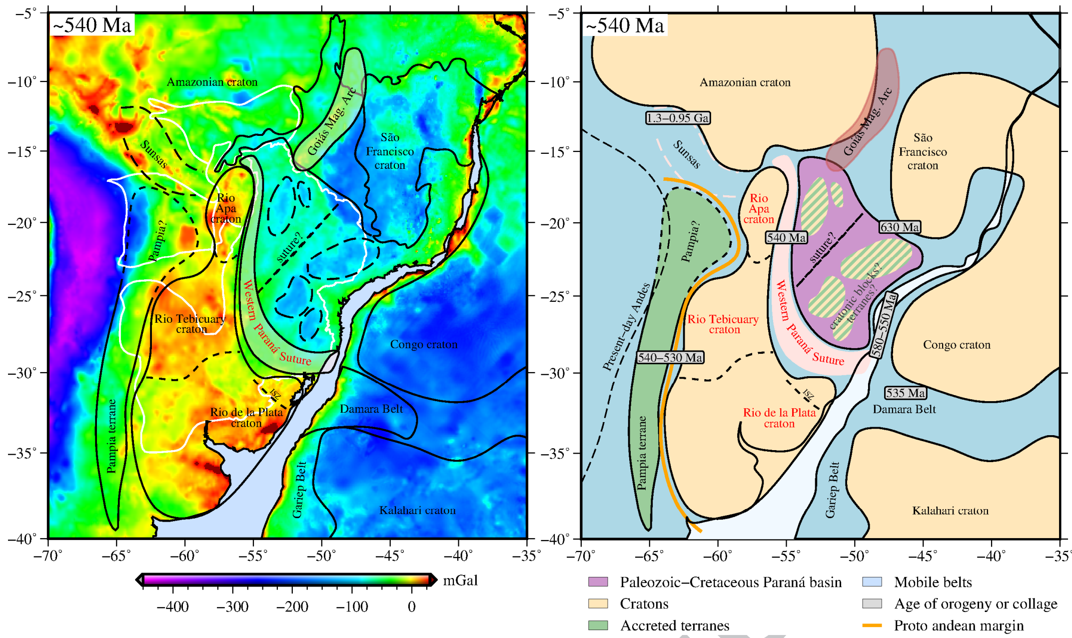
~540 Ma
Amazonian craton
Sunsas
Pampia?
Rio Apa craton
Goiás Mag. Arc
São Francisco craton
suture?
Western Paraná Suture
Rio Tebicuary craton
Rio de la Plata craton
Congo craton
Damara Belt
Gariep Belt
Kalahari craton
Pampia terrane
mGal
−400
−300
−200
−100
0
1.3–0.95 Ga
540 Ma
630 Ma
cratonic blocks/ terranes?
580–550 Ma
535 Ma
540–530 Ma
Present-day Andes
Paleozoic−Cretaceous Paraná basin
Cratons
Accreted terranes
Mobile belts
Age of orogeny or collage
Proto andean margin

Research Highlights

Gravity map reveals the Neoproterozoic 2,000 km long Western Paraná suture/shear zone

Geophysical delimitation of the Rio Apa, Rio Tebicuary and Rio de la Plata cratons

Gravity anomalies of the Amazonian and Rio Apa cratons are distinct

New tectonic features of SW Gondwana final amalgamation revealed